Acupuncture and Herbal Medicine

Human pharmacokinetics and drug interaction potential of GuHong: an intravenous herbal formulation for managing ischemic stroke

Qiu-Yue Wang[1,2], Zhen-Zhen Ma[1,2], Jia-Ye Yuan[1,2], Guo-Li Yue[1,2], Yun-Fei Feng[2,3], Xiao-Yan Xia[2,3], Wei-Wei Jia[2], Fei-Fei Du[2], Feng-Qing Wang[2], Xuan Yu[2], Chen Cheng[2], Yü-Hong Huang[4], Xiao-Kai Wang[5], Yi-Mei Zeng[6], Yan-Fen Li[4], Zi-Jing Song[6], Jun-Ling Yang[1,2,3,7,*], Chuan Li[1,2,3,6,7,*]

[1]Graduate School, Tianjin University of Traditional Chinese Medicine, Tianjin, China; [2]State Key Laboratory of Drug Research, Shanghai Institute of Materia Medica, Chinese Academy of Sciences, Shanghai, China; [3]University of Chinese Academy of Sciences, Chinese Academy of Sciences, Beijing, China; [4]Second Affiliated Hospital, Tianjin University of Traditional Chinese Medicine, Tianjin, China; [5]Tonghua Guhong Pharmaceutical Tonghua, China; [6]Zhongshan Institute for Drug Discovery, Zhongshan, China; [7]China-Serbia "Belt and Road" Joint Laboratory for Natural Products and Drug Discovery, Shanghai Institute of Materia Medica, Chinese Academy of Sciences, Shanghai, China

Abstract

Objective: Unlike for drug-drug interactions, rigorous guidelines for assessing herb-drug interactions are nonexistent. GuHong is an intravenous herbal formulation used as adjunct therapy for the management of ischemic stroke. This investigation aimed to evaluate its potential to precipitate pharmacokinetic drug interactions. To facilitate the potential assessment, a human multi-compound pharmacokinetic study, along with associated supportive studies, was conducted to pinpoint GuHong compounds for testing.

Methods: After analyzing the chemical composition of GuHong, a pharmacokinetic study was conducted in healthy subjects who received GuHong intravenously to identify its significantly exposed compounds and their pharmacokinetics. In addition, supportive rat and *in vitro* studies were conducted to assess the hepatic and renal disposition of these compounds, including their metabolism and transport. The potential of GuHong to precipitate drug interactions was evaluated *in vitro* using significantly exposed compounds, which were tested for their effects on drug-metabolizing enzymes and drug transporters listed in the ICH M12 Guideline (2024), with a focus on inhibition and induction. Samples were analyzed by liquid chromatography-mass spectrometry.

Results: A total of 54 constituents (0.01–27.18 μmol/day) derived from *Carthamus tinctorius* flowers (Honghua) and *N*-acetyl-L-glutamine (3,090 μmol/day) were detected in GuHong. Following intravenous administration of GuHong, hydroxysafflor yellow A emerged as the principal circulating compound from Honghua. Saffloquinoside D, kaempferol-3-*O*-rutinoside, kaempferol-3-*O*-sophoroside, 8-hydroxycinnamic acid-8-*O*-glucoside, coumaric acid-4-*O*-glucoside, and chlorogenic acid, also from Honghua, were detected but at low plasma levels. Hydroxysafflor yellow A, primarily eliminated *via* glomerular filtration-based renal excretion, exhibited the characteristics of an intravenous "hard drug." *N*-Acetyl-L-glutamine was another major circulating compound of GuHong and was eliminated through renal excretion and hydrolysis to L-glutamine. GuHong had a low potential to precipitate pharmacokinetic drug interactions.

Conclusions: The low drug interaction potential of GuHong is advantageous for its use in the treatment of ischemic stroke in the context of polypharmacy. The methodology developed here can be applied to the study of other complex herbal medicines for their pharmacokinetic drug interaction potential.

Keywords: *Carthamus tinctorius*, Drug interaction, GuHong injection, Hydroxysafflor yellow A, *N*-Acetyl-L-glutamine, Pharmacokinetics

Graphical Abstract: https://links.lww.com/AHM/A173

Introduction

In China, integrating Chinese medicine with Western medicine to treat many multifactorial diseases is a significant advantage[1–8]. This integration necessitates a high degree of pharmacokinetic compatibility between the complex herbal medicines and the comedicated synthetic drugs, meaning the absence of unintentional pharmacokinetic drug interaction that could interfere with drug therapy leading to decreased efficacy or safety[9–10]. Co-administration of grapefruit juice or St. John's wort formulations has been reported to severely disrupt synthetic drug therapy by, respectively,

*Corresponding author. Jun-Ling Yang and Chuan Li, E-mail: yangjl@simm.ac.cn and chli@simm.ac.cn.

Received 9 October 2024 / Accepted 14 April 2025

How to cite this article: Wang QY, Ma ZZ, Yuan JY, Yue GL, Feng YF, Xia XY, Jia WW, Du FF, Wang FQ, Yu X, Cheng C, Huang YH, Wang XK, Zeng YM, Li YF, Song ZJ, Yang JL, Li C. Human pharmacokinetics and drug interaction potential of GuHong: an intravenous herbal formulation for managing ischemic stroke. Acupunct Herb Med 2025;5(2):173–192. DOI: 10.1097/HM9.0000000000000155

Copyright © 2025 Tianjin University of Traditional Chinese Medicine. This is an open-access article distributed under the terms of the Creative Commons Attribution-Non Commercial-No Derivatives License 4.0 (CCBY-NC-ND), where it is permissible to download and share the work provided it is properly cited. The work cannot be changed in any way or used commercially without permission from the journal.

inhibiting or inducing the cytochrome P_{450} enzyme CYP3A[11–16]. These findings raise concerns about the concurrent use of synthetic drugs and natural products, including herbal medicines[17–22]. To ensure safe and effective drug combination therapy in integrating Chinese medicine with Western medicine, it is essential to clearly articulate the risks associated with pharmacokinetic drug interactions. Although the Guideline on Drug Interactions issued by the Chinese National Medical Products Administration (NMPA) in 2021 highlights the risks of pharmacokinetic drug interactions involving Chinese herbal medicines, it does not provide specific methods for risk assessment (https://www.cde.org.cn/zdyz). The complex chemical composition of Chinese herbal medicines complicates the evaluation of their potential for drug interactions when combined with synthetic drugs. The selection of compounds from a complex herbal medicine for risk assessment is a challenge in such an evaluation. To address this issue, we developed a multi-compound pharmacokinetic approach to identify potentially important herbal compounds that are significantly bioavailable for drug interactions and to characterize their pharmacokinetics and disposition that could affect the occurrence of interactions[10,23–26].

GuHong injection, an intravenous herbal formulation, is licensed by the Chinese NMPA as an adjunct therapy for ischemic stroke and related symptoms. Each milliliter of GuHong comprises an aqueous extract of 0.5 g *Carthamus tinctorius* flowers (known as "Honghua" in Chinese) and 30 mg of *N*-acetyl-L-glutamine. The efficacy of GuHong in treatment of acute ischemic stroke has been demonstrated through a multi-center, randomized, double-blind, placebo-controlled trial, which involved 1,999 patients with acute ischemic stroke[27]; the administration of GuHong alongside conventional management resulted in a higher proportion of patients with 90-day modified Rankin scale (the primary endpoint and long-term outcome measure in stroke trials) of 0 to 2 (73.9%) when compared to conventional management alone (67.5%; $P < 0.001$). Another multi-center clinical trial, which involved 399 patients with acute ischemic stroke, showed that GuHong, when used alongside basic treatment, outperformed butylphthalide in reduction of 14-day National Institute of Health Stroke Scale scores (short-term outcome measure in stroke trials; –2.33 *versus* –1.45, $P < 0.0001$)[28]. Animal studies demonstrated that GuHong facilitated post-stroke functional recovery *via* attenuating cortical inflammation and apoptosis in the subacute stage of ischemic stroke[29–30]. Following the initial treatment of acute ischemic stroke with intravenous thrombolysis within 4.5 hours of symptom onset, subsequent management includes antiplatelet therapy, anticoagulation, lipid-lowering therapy, blood pressure control, glycemic regulation, as well as neuroprotective and supportive interventions[31]. Thus, GuHong, when used in the treatment of acute ischemic stroke, is typically co-administered with various synthetic drugs. Therefore, its potential for pharmacokinetic drug interactions warrants careful assessment.

Unlike synthetic drugs, intravenous GuHong possesses a complex chemical composition[32]. To date, limited human pharmacokinetic investigations have been conducted on GuHong, along with assessments of its potential for pharmacokinetic drug interactions. Several research groups have developed assays for measuring plasma concentrations of the GuHong compounds hydroxysafflor yellow A and *N*-acetyl-L-glutamine over time in rats intravenously administered the herbal medicine[32–36]. To assess the potential of GuHong to precipitate pharmacokinetic drug interactions, a drug combination study was conducted, which was supported by a multi-compound pharmacokinetic study of the herbal medicine. The multi-compound pharmacokinetic study, based on a comprehensive composition analysis of GuHong, was performed to ensure reliable identification of the medicine's potentially important compounds that were significantly bioavailable for precipitating drug interactions. This involved the characterization of these compounds' human plasma pharmacokinetics and disposition (including renal biotransformation of *N*-acetyl-L-glutamine). The findings from this investigation provide valuable insights into the rational clinical application of GuHong.

Materials and methods

GuHong and study materials

GuHong injection was manufactured by Tonghua Guhong Pharmaceutical Co., Ltd. (Tonghua, Jilin Province, China) with the Chinese NMPA drug ratification number of GuoYaoZhunZi-H22026582. Each milliliter of GuHong is prepared from 0.5 g Honghua and 30 mg *N*-acetyl-L-glutamine, and the final product is a sterile and non-pyrogenic formulation for intravenous administration. Samples of six lots of GuHong were obtained from Tonghua GuHong Pharmaceutical to determine the herbal injection's chemical composition and lot-to-lot variability. Honghua (*Carthamus tinctorius* flowers) was also provided by Tonghua GuHong Pharmaceutical. To support the composition analysis of GuHong, the component herb Honghua was pulverized and subjected to ultrasonic-assisted extraction three times with 50% methanol for analysis. A 5% glucose injection (GuoYaoZhunZi-H12020021) was obtained from Otsuka Pharmaceuticals (Dalian, Liaoning Province, China). Reference standards of hydroxysafflor yellow A, kaempferol-3-*O*-sophoroside, kaempferol-3-*O*-rutinoside, coumaric acid-4-*O*-glucoside, *p*-coumaric acid, and chlorogenic acid were purchased from Chroma Biotechnology (Chengdu, Sichuan Province, China). *N*-Acetyl-L-glutamine, adenosine 5′-triphosphate (ATP), and adenosine 5′-monophosphate (AMP) were purchased from Sigma-Aldrich (St. Louis, MO, USA). *N*-Acetyl-DL-glutamine-2,3,3,4,4-d_5 was purchased from Isoreag (Isoscience, King of Prussia, PA, USA). 8-Hydroxycinnamic acid-8-*O*-glucoside was isolated from Honghua and purified with its chemical structure elucidated using a Bruker AVANCE III-500 MHz spectrometer (Bremen, Germany) [Supplementary Table S1, https://links.lww.com/AHM/A174]. The purity of the preceding reference standards and the isolated compound was ≥98%.

Pooled human liver microsomes (HLM) and cytosol (HLC) were obtained from Gentest (Woburn, MA, USA). Pooled human kidney cytosol (HKC) was obtained from XenoTech (Osaka, Japan). Rat liver microsomes (RLM),

rat liver cytosol (RLC), and rat kidney cytosol (RKC) were prepared in-house by differential centrifugation. Plateable cryopreserved primary human hepatocytes from three donors were obtained from Bioreclamation IVT (Baltimore, MD, USA); donor information is summarized in Supplementary Table S2 [https://links.lww.com/AHM/A174]. Acylase I (EC 3.5.1.14, also known as aminoacylase) was purchased from BidePharm (Shanghai, China). Human embryonic kidney 293 (HEK-293) cells were obtained from the American Type Culture Collection (Manassas, VA, USA). Transporter expression plasmids of the human organic anion-transporting polypeptide (OATP)1B1, OATP1B3, organic anion transporter (OAT)1, OAT3, organic cation transporter (OCT)2, multidrug and toxin extrusion protein (MATE)1, and MATE2K were synthesized by Invitrogen Life Technologies (Shanghai, China). Inside-out membrane vesicles (5 mg protein/mL) prepared from insect cells expressing human multidrug resistance (MDR)1, human multidrug resistance-associated protein (MRP)2, human breast cancer resistance protein (BCRP), and human bile salt export pump (BSEP) were purchased from Genomembrane (Kanazawa, Japan).

High-performance liquid chromatography (HPLC)-grade methanol, acetonitrile, and formic acid were obtained from Sigma-Aldrich. HPLC-grade water was prepared in-house using a Millipore Milli-Q Integral 3 Cabinet Water Purifying System (Bedford, MA, USA).

Assay for composition analysis of GuHong

The composition analysis of GuHong was conducted using a Waters Synapt G2 high-definition time-of-flight mass spectrometer (Manchester, UK) coupled with a Waters Acquity ultraperformance liquid chromatographic separation module (Milford, MA, USA) through a LockSpray electrospray ionization (ESI) source.

Before analyzing the chemical composition of GuHong samples, the analyte capacity of an initial chemical profiling (ICP) assay under fixed conditions [Supplementary Information, https://links.lww.com/AHM/A174] was evaluated retrospectively with compounds previously detected and characterized in other herbal medicines[23–26,37–43]. This enabled the comparison of the analyte capacity of the assay with the required analyte capacity for the compositional analysis of GuHong. The required analyte capacity was evaluated using the reported Honghua compounds obtained *via* literature mining. Both analyte capacities were determined in terms of the molecular descriptors of the compounds, including molecular mass (MW), distribution coefficient at pH 7 ($\text{Log}D_{\text{pH7}}$), aqueous solubility at pH 7 ($\text{Log}S_{\text{pH7}}$), hydrogen bond donors plus hydrogen bond acceptors (HBD + HBA), and dissociation constant ($\text{p}K_{\text{a}}$). The molecular descriptors were calculated using ACD/Percepta software (Toronto, ON, Canada). When the descriptor ranges of the required analyte capacity were within the respective ranges of the analyte capacity of the assay, the ICP assay was considered suitable for the composition analysis of GuHong without the need for assay modification or supplementary assays.

Liquid chromatographic (LC) separation was achieved on a 1.7-μm Waters Acquity UPLC BEH C_{18} column (100 mm × 2.1 mm i.d.; Dublin, Ireland) using a mobile phase, consisting of solvent A (water, containing 0.1‰ formic acid) and solvent B (methanol, containing 0.1‰ formic acid). The mobile phase was delivered at 0.3 mL/min using a 42-min gradient program that consisted of 0 to 2 min at 2% solvent B, 2 to 32 min from 2% to 98% solvent B, 32 to 37 min at 98% solvent B, and 37 to 42 min at 2% solvent B. For mass spectrometry (MS) analysis, the ESI source worked in the positive (+3.0 kV) and negative ion modes (–2.5 kV) at 120°C with the sampling cone at 40 V (positive mode) and –30 V (negative mode) and the extraction cone at 5.0 V. The mass spectrometer was operated in sensitivity mode with a resolving power of approximately 10,000 and was externally calibrated with sodium formate over a range of *m/z* 50–1,500. Mass shifts during acquisition were corrected using leucine enkephalin (*m/z* 554.2615 in negative ion mode and *m/z* 556.2771 in positive ion mode). MS^{E} data acquisition (in centroid mode, *m/z* 50–1,500) was achieved using low collision (trap collision energy, 4 V) and high collision energies (ramp trap collision energy, 30–50 V) with a scan time of 0.3 seconds. The chromatograms of the GuHong and Honghua extract were compared and the chromatograms of 50% methanol were used as blanks for subtraction to identify the peaks corresponding to the Honghua constituents in GuHong.

Constituents with known names, structures, and available reference standards were characterized by comparing them to their respective reference standards with respect to LC retention time and MS data. Constituents with known names/structures but unavailable reference standards were characterized by comparing them to literature-mined MS data, as well as LC data. Quantification of the characterized Honghua constituents was performed by calibration with the respective reference standards (when available) or, when necessary, with structurally similar reference standards.

Human pharmacokinetic study of GuHong

A single-center, open-label pharmacokinetic study of GuHong was performed on healthy volunteers at the Second Affiliated Hospital of Tianjin University of Traditional Chinese Medicine (Tianjin, China). The study protocol was reviewed and approved by the Ethics Committee of Clinical Investigation at the hospital. The study was registered at the Chinese Clinical Trials Registry (www.chictr.org.cn) under registration number ChiCTR2100045623 and was performed in accordance with the *Declaration of Helsinki*. A total of 12 healthy volunteers (six men and six women) aged between 20 and 33 years with body mass indices of 20.5 to 23.6 kg/m^2 provided written informed consent before enrollment. The participants were deemed to be in good health based on their medical history, physical examination results, vital signs, electrocardiograms, and clinical laboratory tests. They were required to be non-smokers and not allergic to GuHong. The female volunteers were required to be neither menstruating nor pregnant. The use of synthetic drugs or herbal medicines was prohibited from 2 weeks before the study until its conclusion. Alcoholic beverages were also prohibited from 2 days before the commencement of the study until its conclusion.

Human subjects received a 1.5-hour intravenous infusion of GuHong, for seven consecutive days at the medicine's label dose of 20 mL per day. For dosing, 20 mL GuHong was mixed with 250 mL 5% glucose injection, and the resulting solution was infused through an arm vein using a ZNB-XB intelligent infusion pump (Beijing, China). On day 1, serial blood samples (approximately 1.5 mL each time) were collected using an antecubital vein catheter before and 0.5, 1, 1.5 (just before terminating infusion), 1.583, 2, 2.5, 3.5, 5.5, 7.5, 9.5, and 24 h after starting infusion of GuHong. Serial urine samples were also collected before and at 0 to 3, 3 to 6, 6 to 10, and 10 to 24 h after starting the infusion. On days 2 to 6, blood samples were collected before and 1.5 hours after starting infusion. On day 7, blood and urine samples were collected according to the schedule on day 1. Heparinized blood samples were centrifuged to obtain plasma fractions, which were stored at –70°C until analysis. Urine samples, without any added preservative, were weighed and stored at –70°C pending analysis.

The liver and kidney function of each participant were monitored on day 1 (before GuHong administration), day 4 (before GuHong administration), and day 8. Serum alanine aminotransferase, aspartate aminotransferase, total protein, albumin-to-globulin ratio, total bilirubin, and direct bilirubin were monitored as liver function markers, while serum creatinine and blood urea nitrogen levels were monitored as kidney function markers.

Supportive rat pharmacokinetic studies

Rat pharmacokinetic studies were performed at the Laboratory Animal Center of Shanghai Institute of Materia Medica (Shanghai, China). The study protocols were reviewed and approved by the Institutional Animal Care and Use Committee of the Shanghai Institute of Materia Medica (2020-10-LC-33). The care and use of rats complied with the Guidance for Ethical Treatment of Laboratory Animals (the Ministry of Science and Technology of China, 2006). Male Sprague-Dawley rats (230–280 g) were obtained from Huachuang Sino Pharmaceutical Technology (Taizhou, Jiangsu Province, China). Rats were maintained in a unidirectional airflow room at 20°C to 24°C and relative humidity of 30% to 70% with a 12-hour light/dark cycle. The rats underwent femoral artery cannulation for blood sampling as described previously[44]. After surgery, rats were housed individually and allowed to regain their preoperative body weights before further use. Thirty rats were used in the following four studies.

In the first study, six rats received a bolus dose of 2 mL/kg GuHong intravenously (a dose translated from the human label dose of GuHong using a body surface area normalization method[45]). Serial blood samples (about 150 µL for each time point) were collected before and 5, 15, 30, and 45 min and 1, 1.5, 2, 4, 6, 8, and 24 h after GuHong administration into heparinized tubes. Blood samples were centrifuged to obtain plasma fractions, which were then stored at –70°C until analysis.

In the second study, six rats were housed individually in rat metabolic cages. After intubation with 2 mL water, each rat received a bolus dose of 2 mL/kg GuHong intravenously. Serial urine samples were collected before dosing and at 0 to 8, 8 to 24, 24 to 32, and 32 to 48 h after dosing. The urine samples, without any added preservative, were weighed and stored at –70°C pending analysis.

In the third study, 15 rats received a bolus dose of GuHong intravenously at 2 mL/kg, were sacrificed (three rats per time point) under isoflurane anesthesia by bleeding from the abdominal aorta at 0.08, 0.5, 1, 2, and 4 h after dosing, and perfused with 15-mL saline through the superior vena cava. Blood samples were collected into heparinized tubes and centrifuged to obtain plasma fractions. The livers were excised, rinsed in ice-cold saline, blotted, weighed, and homogenized in fourfold volumes of ice-cold saline. The plasma samples and the liver homogenate samples were stored at –70°C until analysis.

In the fourth study, three rats were intravenously administered a bolus dose of *N*-acetyl-DL-glutamine-2,3,3,4,4-d_5 at 6 mg/kg (1/10 dose of *N*-acetyl-L-glutamine in GuHong). Serial blood samples (approximately 150 µL for each time point) were collected before and 5, 15, 30, and 45 min and 1, 1.5, 2, 4, 6, 8, and 24 h after dosing into heparinized tubes. Blood samples were centrifuged to obtain plasma fractions, which were then stored at –70°C until analysis.

Supportive in vitro metabolism studies

To assess the metabolism potential of intravenous hydroxysafflor yellow A, several *in vitro* metabolism studies were conducted by incubating the compound with reduced nicotinamide adenine dinucleotide phosphate (NADPH)-fortified RLM and HLM (for cytochrome P450-mediated oxidation; midazolam used as positive substrate), reduced nicotinamide adenine dinucleotide (NADH)-fortified RLC and HLC (for aldehyde dehydrogenase-mediated oxidation; protocatechuic aldehyde), uridine 5′-diphospho-glucuronic acid (UDPGA)-fortified RLM and HLM (for uridine diphosphate-glucuronosyltransferase-mediated glucuronidation; chrysin), 3′-phosphoadenosine-5′-phosphosulfate (PAPS)-fortified RLC and HLC (for sulfotransferase-mediated sulfation; 7-hydroxyflavone), or glutathione (for glutathione conjugation), under the conditions for the metabolic reactions as described previously[39–40]. Furthermore, two-step metabolism was assessed for hydroxysafflor yellow A, that is, P450-mediated oxidation followed by catechol-*O*-methyltransferase-mediated methylation and P450-mediated oxidation followed by glutathione conjugation. Given that intravenous hydroxysafflor yellow A is poorly excreted into bile, intestinal microbiota-mediated reduction or dehydration was not considered for this compound. Moreover, hydroxysafflor yellow A does not contain a catechol moiety or nitrogen atom; therefore, neither catechol-*O*-methyltransferase-mediated methylation nor *N*-acetyltransferase-mediated acetylation was considered for this compound.

The comparative deacetylation of *N*-acetyl-L-glutamine into L-glutamine by hepatic and renal acylases was assessed using acylase I, human liver cytosol, human kidney cytosol, rat liver cytosol, and rat kidney cytosol fortified with 0.5 mmol/L $CoCl_2$. The metabolic reaction was initiated by adding *N*-acetyl-L-glutamine or *N*-acetyl-DL-glutamine-2,3,3,4,4-d_5 into acylase I

or cytosols (final concentration of 200 μmol/L) at 37°C and terminating the reaction at 0, 15, and 30 min and 1 and 2 h by adding three volumes of ice-cold acetonitrile. *N*-Acetyl-L-methionine was used as the positive substrate.

Supportive in vitro transport studies

To assess the potential involvement of transporters in the distribution and elimination of GuHong compounds, the cellular uptake of these compounds at a concentration of 20 μmol/L was investigated in HEK-293 cells that were transiently transfected with human OAT1, OAT2, OAT3, OATP1B1, and OATP1B3 and rat Oatp1b2 and Oat2. The transporter expression plasmid was introduced into the HEK-293 cells using Lipofectamine 2000 (Invitrogen, Carlsbad, CA, USA). Cell culture and transport studies were performed as previously described[46–47]. Differential uptake between transfected cells (TC) and mock cells (MC) was defined as the net transport ratio ($Transport_{TC}$/$Transport_{MC}$). A net transport ratio >3 indicated that the test compound was a substrate of the transporter. Before use, the transfected cells were functionally characterized by measuring the uptake of *para*-aminohippuric acid, prostaglandin F_{2a}, estrone-3-sulfate, and estradiol-17-β-D-glucuronide for OAT1, OAT2/Oat2, OAT3, and OATP1B1/OATP1B3/Oatp1b2, respectively.

Inside-out membrane vesicles expressing human MDR1, MRP2, BCRP, or BSEP, or rat Mrp2, Bcrp, or Bsep were tested with GuHong compounds, each at 20 μmol/L, using a rapid filtration method as described previously[47]. ATP was used as the energy source to transport the test compounds across the vesicle membrane, and AMP was used as a negative control. ATP-dependent transport was defined as the net transport ratio ($Transport_{ATP}$/$Transport_{AMP}$ ratio). A net transport ratio >3 indicated that the test compound was a substrate of the transporter. The vesicles were functionally characterized using ginsenoside Rg_1, estradiol-17β-D-glucuronide, methotrexate, and taurocholic acid as a substrate for MDR1, MRP2/Mrp2, BCRP/Bcrp, and BSEP/Bsep, respectively.

In vitro assessment of the significantly in vivo-exposed compounds of GuHong for inhibition of drug-metabolizing enzymes and drug transporters

The potential of GuHong to precipitate drug interactions was evaluated *in vitro* using significantly *in vivo*-exposed compounds, which were tested for their inhibition of drug-metabolizing enzymes and drug transporters listed in the International Council for Harmonization of Technical Requirements for Pharmaceuticals for Human Use (ICH) M12 Guideline titled "Drug Interaction Studies" (https://database.ich.org/sites/default/files/ICH_M12_Step4_Guideline_2024_0521_0.pdf). The test *in vivo*-exposed GuHong compounds were hydroxysafflor yellow A, kaempferol-3-*O*-rutinoside, kaempferol-3-*O*-sophoroside, 8-hydroxycinnamic acid-8-*O*-glucoside, coumaric acid-4-*O*-glucoside, chlorogenic acid, *N*-acetyl-L-glutamine, and mixture of GuHong compounds (MGHC) (a mixture of the seven GuHong compounds).

The inhibition of human P450 enzymes by the GuHong compounds was assessed using NADPH-fortified HLM. Probe substrates for CYP1A2, CYP2B6, CYP2C8, CYP2C9, CYP2C19, CYP2D6, and CYP3A were phenacetin (50 μmol/L), bupropion (50 μmol/L), amodiaquine (10 μmol/L), diclofenac (10 μmol/L), *S*-mephenytoin (50 μmol/L), dextromethorphan (6 μmol/L), and midazolam/testosterone (2.5/25 μmol/L), respectively. The initial screening of inhibitory activity was conducted at 100 μmol/L for hydroxysafflor yellow A, 10 μmol/L for each of the other test compounds originating from Honghua, 2,000 μmol/L for *N*-acetyl-L-glutamine, and 10,062 μmol/L of a total concentration for MGHC (equivalent to 50-fold of the total unbound C_{max} of human subjects receiving intravenous GuHong at labeled dose). When >50% inhibition was demonstrated in the initial screening test, the half-maximal inhibitory concentration (IC_{50}) was determined for the P_{450} isoenzymes. Time-dependent inhibition was examined using a single-point inactivation method[48].

The GuHong compounds were assessed for their inhibition of human OATP1B1, OATP1B3, OAT1, OAT3, OCT2, MATE1, and MATE2K. Probe substrates for OATP1B1/OATP1B3, OAT1, OAT3, and OCT2/MATE1/MATE2K were estradiol-17-β-D-glucuronide, *para*-aminohippuric acid, estrone-3-sulfate, and tetraethylammonium (10 μmol/L for all), respectively. The initial screening for inhibitory activity was conducted at the concentrations used in the enzyme inhibition study for the test compounds. When >50% inhibition was demonstrated in the initial screening test, the IC_{50} was determined for the transporters.

The ability of the GuHong compounds to inhibit human MDR1 and BCRP was assessed. Probe substrates for MDR1 and BCRP were ginsenoside Rg_1 and methotrexate (10 μmol/L for both), respectively. The initial screening for inhibitory activity was conducted at the concentrations used in the enzyme inhibition study for the test compounds. When >50% inhibition was demonstrated in the initial screening test, the IC_{50} was determined for the transporters.

In vitro assessment of the significantly in vivo-exposed compounds of GuHong for induction of cytochrome P_{450} enzymes

Induction of CYP1A2, CYP2B6, and CYP3A4 by the test GuHong compounds hydroxysafflor yellow A, kaempferol-3-*O*-rutinoside, kaempferol-3-*O*-sophoroside, 8-hydroxycinnamic acid-8-*O*-glucoside, coumaric acid-4-*O*-glucoside, chlorogenic acid, and *N*-acetyl-L-glutamine was assessed using cryopreserved human hepatocytes from three donors (DJJ, NHI and YNS) in triplicate at concentrations of 1-, 5-, and 50-fold of the unbound C_{max} of human subjects receiving intravenous GuHong at labeled dose, while for MGHC the test concentrations was 1-, 5-, and 50-fold of total unbound C_{max}. Cell culture and induction studies were performed as previously described[9,26]. The negative control was a 0.08% DMSO solution. Positive inducers for CYP1A2, CYP2B6, and CYP3A4 were omeprazole (50 μmol/L), phenobarbital (1 mmol/L), and rifampin (20 μmol/L), respectively. Fold induction was calculated using both enzyme activity

and mRNA levels. The probe substrates for CYP1A2, CYP2B6, and CYP3A4 were phenacetin (100 μmol/L), bupropion (250 μmol/L), and midazolam (8 μmol/L), respectively. Differential enzyme activity between treated and untreated cells was defined as the treated/untreated cell ratio of enzyme activity (EA-T/U ratio) by measuring metabolite concentrations. A ratio of ≥2 for a test compound and a ratio of ≥20% of the positive control from at least one of the three donors indicated a positive induction. Cellular enzyme mRNA levels were determined by SYBR-based quantitative real-time polymerase chain reaction (qRT-PCR) analysis. The relative quantity of the target mRNA was determined using the ΔΔCt method. For the test compound, a ratio of enzyme mRNA levels between the treated and untreated cells (mRNA-T/U ratio) of ≥4 from at least one of the three donors indicated a positive result.

Assays for bioanalysis of GuHong compounds and study-related compounds in biosamples

To facilitate the pharmacokinetic investigation of GuHong, four types of bioanalysis were performed: (1) profiling of Honghua compounds (unchanged and metabolized) in biosamples; (2) quantification of significantly *in vivo*-exposed compounds originating from Honghua in biosamples; (3) quantification of *N*-acetyl-L-glutamine, L-glutamine, *N*-acetyl-DL-glutamine-2,3,3,4,4-d_5 and L-glutamine-2,3,3,4,4-d_5 in biosamples; (4) quantification of index substrates or their metabolites in biosamples.

Profiling of GuHong compounds (unchanged and metabolized) in human and rat biosamples was conducted under the same conditions as those used for composition analysis. Biosamples were prepared by precipitation with three volumes of methanol, and the supernatants obtained after centrifugation were used for analysis. The detection and characterization of unchanged GuHong compounds in the biosamples were achieved using the characterized sample of GuHong injection as a reference standard. The detection of metabolized compounds mainly focused on those derived from the major GuHong constituents, and candidate metabolite lists guiding detection were generated using the Accelrys metabolite database (version 2015.1; San Diego, CA, USA). Quantification of GuHong compounds (unchanged and metabolized) in the biosamples was achieved by calibration with the respective reference standards (when available) or, when necessary, with structurally similar reference standards.

Quantification of significantly *in vivo*-exposed compounds originating from Honghua in biosamples was conducted on a TSQ Vantage mass spectrometer (Thermo Fisher, San Jose, CA, USA), interfaced *via* an HESI source with an Agilent 1290 infinity LC system (Waldbronn, Germany). Biosamples were prepared by precipitation with three volumes of methanol, and the supernatants obtained after centrifugation were used for analysis. LC separation was achieved on a 3-μm CAPCELL PAK C18 MGII column (50 mm × 2 mm i.d.; Osaka, Japan) using a mobile phase, consisting of solvent A (water, containing 2.5 mmol/L formic acid) and solvent B (methanol, containing 2.5 mmol/L formic acid). The mobile phase was delivered at 0.3 mL/min using a 10-minute gradient program that consisted of 0 to 0.5 min at 2% solvent B, 0.5 to 7 min at 2% to 70% solvent B, 7.1 to 8 min at 70% to 98% solvent B, and 8.1 to 10 min at 2% solvent B. For MS analysis, the ESI source worked in the negative ion mode with optimal precursor-to-product ion pairs for multiple reaction monitoring of hydroxysafflor yellow A (**1**), saffloquinoside D (**2**), kaempferol-3-*O*-rutinoside (**21**), kaempferol-3-*O*-sophoroside (**22**), 8-hydroxycinnamic acid-8-*O*-glucoside (**51**), coumaric acid-4-*O*-glucoside (**52**), chlorogenic acid (**53**), at *m/z* 611.0 → 491.1, 611.0 → 491.15, 593.2 → 284.5, 609.1 → 449.1, 325.1 → 119.1, 325.0 → 119.1, 353.0 → 191.0, respectively. Quantification of these significantly *in vivo*-exposed compounds in biosamples was achieved by matrix-matched calibration with the respective reference standards, except for **2**, which was calibrated with the structurally similar reference standard hydroxysafflor yellow A. The calibration curves exhibited good linearity ($r^2 > 0.99$). Assay validation was performed according to the ICH M10 Guideline. The lower limit of quantification in human plasma was 9.77 nmol/L for **21**, **22**, 19.53 nmol/L for **1**, **2**, **51**, **52**, and **53**. The intra-batch accuracy and precision were 86% to 114% and 1.2% to 14.4%, respectively, for human plasma, and 90% to 114% and 1.1% to 14.2%, respectively, for human urine. The inter-batch accuracy and precision were 86% to 110% and 3.5% to 20.0%, respectively, for human plasma and 91% to 114% and 1.3% to 18.1%, respectively, for human urine. The coefficients of variation reflecting the matrix effects were 2.5% to 14.1% for human plasma and 3.1% to 15.0% for human urine. Analyte stability under conditions mimicking the analytical process was also evaluated in human plasma and urine, including storage at room temperature for 4 h, storage in an autosampler for 24 h, and three freeze-thaw cycles. The analytes were stable under the test conditions, as indicated by the measured mean concentrations fluctuating within 85% to 114% and 88% to 114% of the nominal concentrations for human plasma and urine, respectively. Carryover in the blank sample, following the upper limits of quantification, was negligible for these analytes. All preceding validation results suggested that the assay was reliable and reproducible for the intended use.

Quantification of *N*-acetyl-L-glutamine (**81**), L-glutamine, *N*-acetyl-DL-glutamine-2,3,3,4,4-d_5, and L-glutamine-2,3,3,4,4-d_5 in the biosamples was also conducted using a TSQ Vantage mass spectrometer interfaced *via* an HESI source with an Agilent 1290 infinity LC system. Biosamples were prepared by precipitation with three volumes of acetonitrile and the supernatants obtained after centrifugation were used for analysis. LC separation was achieved on a 3-μm Luna HILIC column (50 mm × 3 mm i.d.; Torrance, CA, USA) using a mobile phase, consisting of solvent A (water, containing 10 mmol/L ammonium formate and 37.5 mmol/L formic acid), and solvent B (water/acetonitrile, 5:95, containing 2 mmol/L ammonium formate and 37.5 mmol/L formic acid). The mobile phase was delivered at 0.3 mL/min using a 15-minute gradient program consisting of 0 to 6 min at 95% to 90% solvent B, 6.1 to 10 min at 70% solvent B, and 10.1 to 15 min at 95% solvent B. For MS analysis, the ESI source worked in the

positive ion mode with optimal precursor-to-product ion pairs for multiple reaction monitoring of **81**, L-glutamine, *N*-acetyl-DL-glutamine-2,3,3,4,4-d_5, and L-glutamine-2,3,3,4,4-d_5 at *m/z* 189.1 → 130.0, 147.0 → 130.0, 194.1 → 135.0, and 152.0 → 135.0, respectively. Quantification of these compounds in the biosamples was achieved using matrix-matched calibration with the respective reference standards. The calibration curves exhibited good linearity ($r^2 > 0.99$). Assay validation was performed according to the ICH M10 Guideline, demonstrating that the assay was reliable and reproducible for the intended use. In addition, chiral chromatographic separation for levorotatory and the dextrorotatory enantiomers of *N*-acetyl-DL-glutamine-2,3,3,4,4-d_5 was achieved on a 3-µm chiralpak ZWIX(-) column (150 mm × 3 mm i.d.; Illkirch, France) using a mobile phase, consisting of solvent A (water, containing 10 mmol/L ammonium formate and 25 mmol/L formic acid) and solvent B (acetonitrile/methanol, 65:35, containing 10 mmol/L ammonium formate and 25 mmol/L formic acid). The mobile phase was delivered at 0.3 mL/min using a 7-minute gradient program that consisted of 0 to 3 min at 100% solvent B, 3.1 to 5 min at 60% solvent B, and 5.1 to 7 min at 100% solvent B.

Quantification of index substrates or their metabolites in the biosamples was conducted using assays detailed by Zhong et al.[49] and Li et al.[9].

Data processing

Each detected constituent has a two-digit compound ID number in bold. "**01–19**," "**21–49**," "**51–59**," "**61–69**," "**71–79**," and **81** are used to indicate quinochalcones, flavonoids of other types, phenolic acids, nucleotides and nucleobase, spermidines, and *N*-acetyl-L-glutamine, respectively, that is, compound class to which the constituent belongs. All Honghua constituents were ranked in descending order based on their respective daily doses and graded as 10 to 100, 1 to 10, and 0.01 to 1 µmol/day. The compound dose was calculated as the product of their content level (µmol/L) in GuHong and the injection's label daily dose of 0.02 L/day. Constituents with a daily dose <0.01 µmol/day were excluded from subsequent analysis because they are unlikely to achieve pharmacologically significant exposure in the body, whether in their original form or as metabolites, post-administration.

Pharmacokinetic parameters were calculated *via* non-compartmental analysis using the Thermo Kinetica software package (version 5.0; InnaPhase, Philadelphia, PA, USA). IC_{50} values were calculated using the GraFit software (version 5.0; Erithacus Software, Surrey, UK).

All data are expressed as the mean ± standard deviation. Statistical analyses were performed using the IBM SPSS Statistics software (version 19.0; IBM, Somers, NY, USA). Statistical significance was set at $P < 0.05$.

Results

Constituents of GuHong

Based on literature mining, a total of 163 constituents across seven classes were reported for Honghua (*Carthamus tinctorius* flowers), that is, 97 flavonoids (including quinochalcones, flavanols, flavones, flavonones, chalcones), nine phenolic acids, 11 organic acids, 12 nucleosides/nucleobase, 25 alkaloids, six spermidines, and three lignans. Articles by Zhou et al.[50], Zhang et al.[51], Xian et al.[52], Yang et al.[53], and Yao et al.[54] provided the most information about Honghua constituents. The information was used to help analyze the composition of GuHong by generating a candidate compound list, which was also used to validate the suitability of the ICP assay for the intended use. As shown in Figure 1, the ICP assay was suitable for composition analysis of GuHong, as indicated by the assay analyte capacity exceeding the required analyte capacity with respect to MW, LogD_{pH7}, LogS_{pH7}, HBD + HBA, and pK_a.

A total of 54 Honghua constituents with compound doses of ≥0.01 µmol/day were detected and characterized in samples of GuHong (Figure 2; detailed information is shown in Supplementary Table S3, https://links.lww.com/AHM/A174). The constituents comprised 11 quinochalcones (**1–11**), 24 flavonoids of other types (**21–44**), nine phenolic acids (**51–59**), seven nucleotides

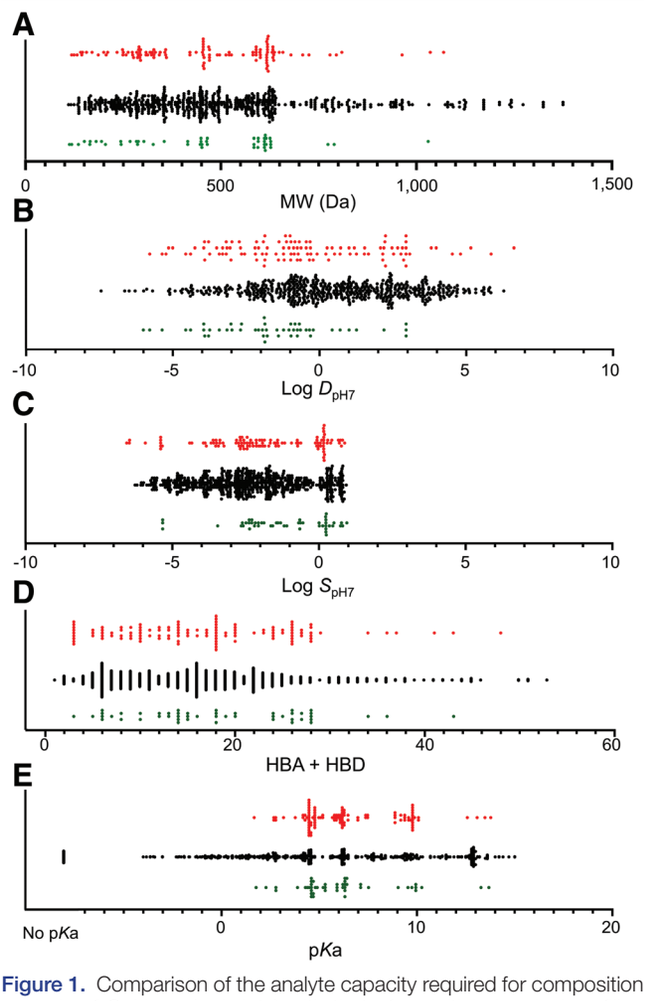


Figure 1. Comparison of the analyte capacity required for composition analysis of GuHong (red dots) with that of an initial chemical profiling assay under fixed conditions [Supplementary Information, http://links.lww.com/AHM/A174; black dots], as well as detected GuHong constituents (green dots). (A) MW; (B) LogD_{pH7}; (C) LogS_{pH7}; (D) HBD + HBA; (E), dissociation constant (pK_a). HBD + HBA: Hydrogen bond donors + hydrogen bond acceptors; LogD_{pH7}: Distribution coefficient at pH 7; LogS_{pH7}: Aqueous solubility at pH 7; MW: Molecular mass.

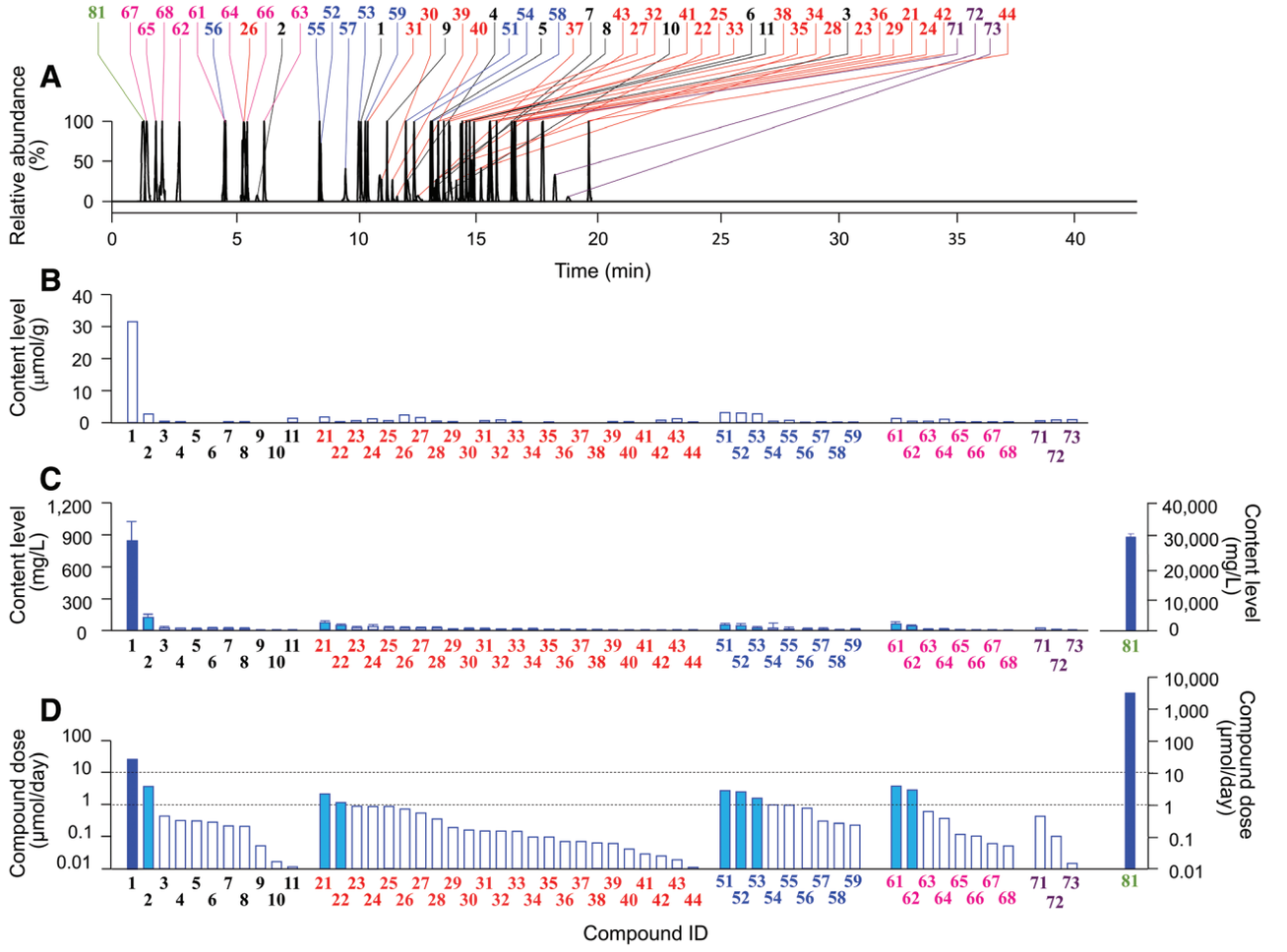


Figure 2. Constituents detected in GuHong. (A) Stacked liquid chromatograms of GuHong constituents, ie, quinochalcones and related constituents (**1–12**), flavonoids of other types (**21–43**), phenolic acids (**51–59**), nucleotides (**61–68**), spermidines (**71–73**), and *N*-acetyl-L-glutamine (**81**) detected by mass spectrometry in a typical sample of GuHong. (B) Constituents detected in a sample of raw material of Honghua (*Carthamus tinctorius* flowers); (C) mean content levels of the GuHong constituents in samples of six lots of GuHong; (D) compound doses (μmol/day) of the GuHong constituents at the label dose of the medicine at 20 mL/day. The names of the GuHong constituents are listed in Supplementary Table S3, https://links.lww.com/AHM/A174.

and nucleobases (**61–67**), and three spermidines (**71–73**). Hydroxysafflor yellow A (**1**; 27.2 μmol/day) was the most abundant Honghua constituent, while guanosine (**61**), saffloquinoside D (**2**), uridine (**62**), 8-hydroxycinnamic acid-8-*O*-glucoside (**51**), coumaric acid-4-*O*-glucoside (**52**), kaempferol-3-*O*-rutinoside (**21**), kaempferol-3-*O*-sophoroside (**22**), and chlorogenic acid (**53**) had lower compound doses (1.0–3.8 μmol/day). *N*-Acetyl-L-glutamine (**81**) in GuHong had a compound dose of 3090 μmol/day. GuHong exhibited lot-to-lot variations of 11.3%, 6.9% to 22.3%, 3.3% to 35.4%, and 3% for **1**, **61/2/62/51/52/21/22/53**, the remaining Honghua constituents, and **81**, respectively.

In vivo-exposed Honghua compounds and their pharmacokinetics after intravenous administration of GuHong

No serious adverse events occurred during the pharmacokinetic study. Seven unchanged Honghua constituents of the flavonoid and phenolic acid classes were detected and characterized in human plasma and urine samples collected after the intravenous administration of GuHong. These circulating compounds were hydroxysafflor yellow A (**1**), saffloquinoside D (**2**), kaempferol-3-*O*-rutinoside (**21**), kaempferol-3-*O*-sophoroside (**22**), 8-hydroxycinnamic acid-8-*O*-glucoside (**51**), coumaric acid-4-*O*-glucoside (**52**), and chlorogenic acid (**53**) (Table 1 and Figure 3). Among these Honghua compounds, **1** exhibited a significantly higher level of systemic exposure (plasma AUC) than the other circulating compounds. No significant metabolites were detected for these compounds in human plasma or urine samples after the administration of GuHong. Other Honghua constituents, including guanosine (**61**), uridine (**62**), or those with a compound dose <1 μmol/day, were not detected in the human plasma or urine samples.

Figure 4 shows the human plasma concentration-time profiles of **1**, **2**, **21**, **22**, **51**, **52**, and **53** after intravenous administration of GuHong, and Table 2 summarizes their pharmacokinetic parameters. All these Honghua compounds exhibited small apparent distribution volumes (V_{SS}, 0.12–0.46 L/kg); this was due, at least in part, to their poor membrane permeability. The total plasma clearance ($CL_{tot,p}$) values of **1** and **2** were significantly lower than that of **52**, which were in turn significantly lower than those of **21**, **22**, **51**, and **53**. The elimination of **1**, **2**, and **52** was based on renal excretion, with

Table 1

Human and rat *in vivo*-exposed GuHong compounds following intravenous administration of the medicine

ID	Compound	LC/TOF-MSE data					Molecular mass (Da)	Presence in human samples	Presence in rat samples
		t_R (min)	ESI_+ (*m/z*)	ESI_- (*m/z*)	Mass error (ppm)	Fragmentation profile (*m/z*)			
1	Hydroxysafflor yellow A	9.88	613.1794	611.1569	–7.0	491.0982, 403.0634, 325.0155, 283.0128	612.1690	Plasma, urine	Plasma, urine, liver
2	Saffloquinoside D	6.35	—	611.1592	–3.3	491.1145, 429.1456, 328.0529, 207.0078, 116.0604	612.1690	Plasma, urine	Plasma, urine, liver
21	Kaempferol-3-*O*-rutinoside	17.23	595.1651	593.1512	0.8	446.9369, 285.0384, 174.9552	594.1585	Plasma, urine	Plasma, urine, liver
22	Kaempferol-3-*O*-sophoroside	14.76	—	609.1440	–2.6	429.0671, 304.9147, 284.0322, 174.9561	610.1534	Plasma, urine	Plasma, urine, liver
51	8-Hydroxycinnamic acid-8-*O*-glucoside	12.32	349.0928	325.0923	–0.3	163.0484, 119.0596	326.1002	Plasma, urine	Plasma, urine, liver
52	Coumaric acid-4-*O*-glucoside	8.13	349.0911	325.0942	5.5	242.9409, 163.0319, 119.0306	326.1002	Plasma, urine	Plasma, urine, liver
53	Chlorogenic acid	9.55	—	353.0864	–2.5	258.9162, 190.9862, 163.0101, 118.9577	354.0951	Plasma, urine	Plasma, urine, liver
81	N-Acetyl-L-glutamine	1.14	189.0881	187.0720	3.2	172.0613, 130.6514, 84.0444	188.0797	Plasma, urine	Plasma, urine, liver

ESI: Electrospray ionization; LC/TOF-MSE: Liquid chromatography/time-of-flight mass spectrometry in the MSE mode.

fractions of doses excreted into urine ($f_{e\text{-}u}$) ranging from 79.4% to 95.6% (mainly *via* glomerular filtration), and their differences in $CL_{tot,p}$ appeared to be associated with their unbound fractions in plasma (f_u). Unlike these compounds, **21** and **22** were likely eliminated mainly *via* hepatobiliary excretion (mediated by OATP1B1/1B3 for sinusoidal uptake and MDR1/BCRP/MRP2 for canalicular efflux; Table 3), whereas their renal clearance (CL_R, mediated by tubular secretion *via* OAT1/2/3) accounted for only 7.9% to 14.4% of the respective $CL_{tot,p}$. Renal excretion of **51** and **53** was also significant ($f_{e\text{-}u}$, 54.8%–65.8%) and appeared to involve tubular secretion, which could be mediated by OAT1/2/3 (Table 3). Hepatobiliary excretion, mainly mediated by OATP1B3 for sinusoidal uptake, might also contribute to the elimination of **51** and **53**. Owing to the joint differences in V_{SS} and $CL_{tot,p}$, **1** had a longer mean elimination half-life ($t_{1/2}$, 3.9 hours) than the other Honghua compounds (<1.7 hours); **21** and **22** exhibited very short $t_{1/2}$ (<5 minutes). No significant accumulation of circulating Honghua compounds occurred during the seven consecutive days of repeated doses of GuHong. No significant sex differences were observed in the human pharmacokinetics of Honghua compounds (Table 2).

To predict human liver exposure to Honghua compounds, additional studies were conducted in rats. Before using the rat liver exposure data, an interspecies comparison was performed, showing comparable plasma and urinary pharmacokinetics of Honghua compounds in rats and humans following intravenous administration of GuHong (Figure 3 and Table 1). To enable a more precise interspecies comparison, the transporter-mediated hepatic disposition was evaluated *in vitro* using both rat and human transporters (Table 3). The effects of the rat transporters on the hepatic disposition of the flavonoids hydroxysafflor yellow A (**1**), saffloquinoside D (**2**), kaempferol-3-*O*-rutinoside (**21**), and kaempferol-3-*O*-sophoroside (**22**) were comparable to those of their human counterparts. Hepatic uptake of the phenolic acids 8-hydroxycinnamic acid-8-*O*-glucoside (**51**) and chlorogenic acid (**53**) could be mediated by human OATP1B3 and OAT2 and by rat Oat2. For coumaric acid-4-*O*-glucoside (**52**), neither human nor rat transporters mediated its hepatic uptake. As shown in Figure 3, the tissue distribution study in rats indicated that all major circulating Honghua compounds exhibited significant liver exposure, whereas Honghua compounds with limited or negligible presence in the bloodstream were similarly undetectable in the liver. Among the major circulating compounds, **1** and **2** exhibited lower liver exposure levels than their respective systemic exposure levels, whereas **21** and **22** exhibited higher liver exposure levels than their respective systemic exposure levels. Honghua compounds **51**, **52**, and **53** exhibited liver exposure levels comparable to their respective systemic exposure levels.

N-Acetyl-L-glutamine metabolism after intravenous GuHong administration

Figure 5 shows the human plasma concentration-time profile of *N*-acetyl-L-glutamine (**81**) after the intravenous administration of GuHong, and Table 4 summarizes its pharmacokinetic parameters. Approximately 36% of dosed **81** were eliminated unchanged *via* renal excretion with a mean renal clearance ratio (R_{rc}) of 0.3. The *in vitro* metabolism study suggested that *N*-acetyl-L-glutamine could be hydrolyzed into L-glutamine by acylase I, the metabolic activity of which was higher in the human kidney cytosol than in the human liver cytosol (Figure 5). Similarly, rat kidney cytosol exhibited higher acylase I activity against *N*-acetyl-L-glutamine than rat liver cytosol. Given that poor membrane permeability (log $D_{pH7.4}$, –0.4) limits passive tubular reabsorption of

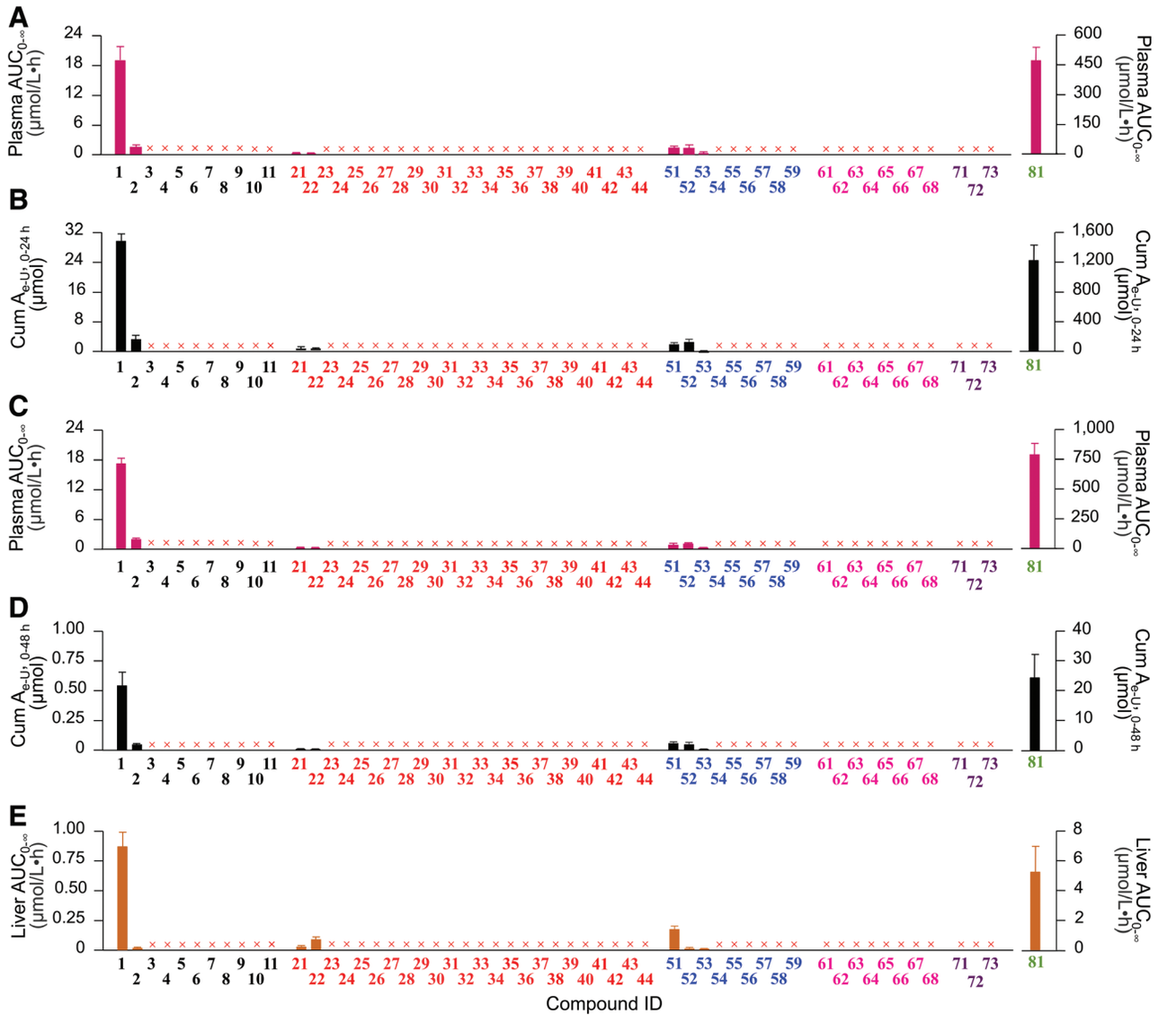


Figure 3. Human and rat *in vivo*-exposed GuHong compounds following intravenous administration of the medicine. (A and C) Human and rat systemic exposure data, respectively; (B and D) human and rat renal excretion data, respectively; and (E) rat liver exposure data. The detection information for these GuHong compounds is shown in Table 1.

N-acetyl-L-glutamine, renal hydrolysis was likely the reason for the low R_{rc} of **81**. Although L-glutamine is a metabolite of **81**, no distinct dose-dependent ascending-descending plasma concentration–time profile of L-glutamine was observed in human subjects following the intravenous infusion of GuHong. Endogenous L-glutamine in human subjects was found at plasma concentrations ranging from 189 to 358 μmol/L. To better understand the *in vivo* hydrolysis of **81** into L-glutamine, *N*-acetyl-DL-glutamine-2,3,3,4,4-d$_5$ was used for *in vitro* and *in vivo* studies, and the samples were analyzed using chiral LC separation. *N*-acetyl-L-glutamine-2,3,3,4,4-d$_5$ was metabolically unstable when incubated with rat kidney cytosol, resulting in the formation of L-glutamine-2,3,3,4,4-d$_5$, whereas *N*-acetyl-D-glutamine-2,3,3,4,4-d$_5$ remained stable without the detection of D-glutamine-2,3,3,4,4-d$_5$ (Figure 5). Following the intravenous administration of *N*-acetyl-DL-glutamine-2,3,3,4,4-d$_5$ to rats, L-glutamine-2,3,3,4,4-d$_5$ displayed a xenobiotic plasma concentration–time profile with a mean $t_{1/2}$ of 1.1 hours (Figure 5 and Table 4).

There were interspecies similarities in the plasma and urinary pharmacokinetics of *N*-acetyl-L-glutamine (**81**), as well as in the impact of transporters on hepatic disposition between rats and humans (Figure 3 and Tables 1 and 3).

Potential of GuHong to precipitate pharmacokinetic drug interactions

To assess GuHong for its potential to perpetrate drug interactions, the major *in vivo*-exposed GuHong compounds (including *N*-acetyl-L-glutamine) and their combination, MGHC, were tested for their inhibition and induction of drug-metabolizing enzymes and transporters listed in the ICH M12 Guideline. No significant inhibition of human cytochrome P_{450} enzymes (CYP1A2, CYP2B6, CYP2C8, CYP2C9, CYP2C19, CYP2D6, CYP3A), SLC transporters (OATP1B1, OATP1B3, OAT1, OAT3, OCT2, MATE1, and MATE2K), or ABC transporters (MDR1 and BCRP) was observed for individual compounds (<50% inhibition at 100 μmol/L of **1**, at 10 μmol/L of **21**, **22**, **51**, **52**, **53** and at 2,000 μmol/L

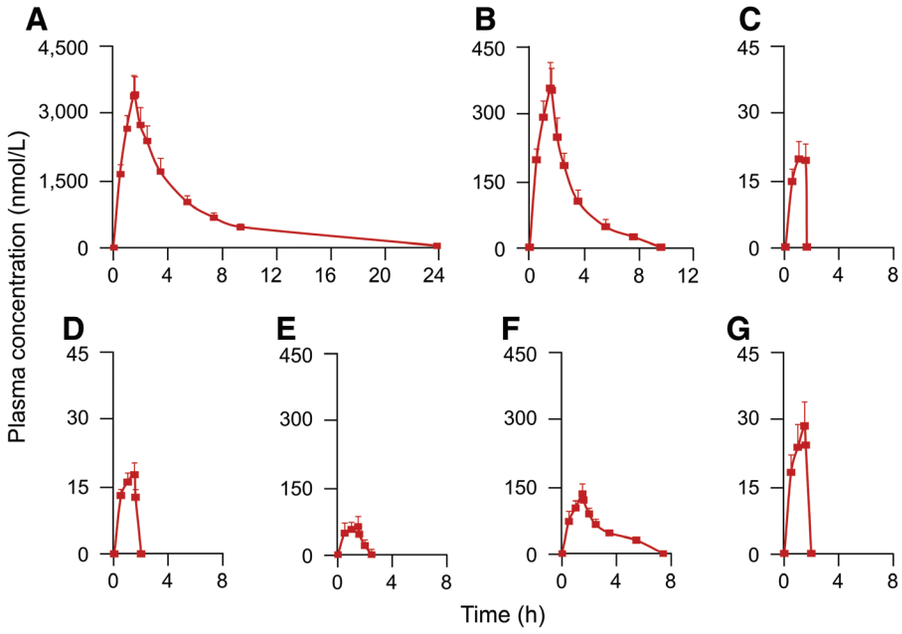


Figure 4. Human plasma concentration–time profiles of Honghua compounds following a single 1.5-h intravenous infusion of GuHong at 20 mL/person/day ($n = 6$). (A–G) Hydroxysafflor yellow A (**1**), saffloquinoside D (**2**), kaempferol-3-*O*-rutinoside (**21**), kaempferol-3-*O*-sophoroside (**22**), 8-hydroxycinnamic acid-8-*O*-glucoside (**51**), coumaric acid-4-*O*-glucoside (**52**), and chlorogenic acid (**53**), respectively.

of **81**) and MGHC (<50% inhibition at a total concentration of 10,062 μmol/L) (Table 5). Regarding cytochrome P_{450} enzyme induction, none of the individual GuHong compounds demonstrated significant induction activity at any of the three concentrations tested (1-, 5-, and 50-fold of the unbound C_{max} in human subjects). However, MGHC, at a total concentration of 10,062 μmol/L (50-fold of the unbound C_{max}), showed positive induction of both CYP2B6 and CYP3A4 in one donor, as evidenced by increased enzyme activity and mRNA expression levels. In contrast, at lower concentrations of 201 and 1,006 μmol/L (1- and 5-fold of the unbound C_{max}), MGHC did not induce significant enzyme activity or mRNA expression (Figure 6 and Supplementary Figure S2, https://links.lww.com/AHM/A174).

Discussion

In China, herbal medicines are often used in combination with synthetic drugs to enhance therapeutic outcomes, such as improving efficacy or reducing toxicity[1–8]. Furthermore, patients with multiple comorbidities are frequently prescribed numerous medications, a practice known as polypharmacy. A key challenge in such combinations is minimizing pharmacokinetic drug interactions, which can result in therapeutic failure. Given the prevalence of drug interactions in clinical practice, ICH issued the M12 Guideline on *Drug Interaction Studies* in 2024. Drug interactions precipitated by natural products, including herbal medicines, also pose a significant concern in clinical settings[17–22]. However, the ICH guideline does not offer specific recommendations regarding which compounds of a complex herbal medicine that should be selected to assess the potential of the medicine to precipitate pharmacokinetic drug interactions. To address this gap, a multi-compound pharmacokinetic methodology has been developed to prioritize the *in vivo*-exposed compounds of herbal medicines for drug interaction studies[10,23–24]. With respect to the metabolizing enzymes and transporters highlighted in the ICH guideline, which are commonly involved in intestinal drug absorption and/or disposition, the *in vivo*-exposed compounds are those that exhibit significant exposure levels in the intestinal lumen, systemic circulation, and/or liver. For intravenous herbal medicines, such as GuHong, both systemic and liver exposure levels are critical for assessing their potential to precipitate drug interactions. For example, systemic exposure is associated with transporters, such as hepatic OATP1B1, OATP1B3, and OCT2, as well as renal OAT1, OAT3, and OCT2, whereas liver exposure is linked to the hepatic P450 enzymes CYP1A2, CYP2B6, CYP2C8, CYP2C9, CYP2C19, CYP2D6, and CYP3A, as well as hepatic P-gp, BCRP, and MATE1. It is worth noting that systemic and liver exposure can differ substantially. For instance, significant liver exposure may be present with negligible systemic exposure, as well as notable differences in metabolite-to-precursor ratios between the two exposure sites[55–56]. This discrepancy arises because the liver exposure is influenced by hepatic drug transporters and/or metabolizing enzymes. While human systemic exposure data can be obtained directly through clinical pharmacokinetic studies, human liver exposure data are typically unavailable from such studies. In this investigation, systemic exposure data were obtained from a human pharmacokinetic study of GuHong. To assess liver exposure, additional studies were conducted using rats. Before using the rat liver exposure data, an interspecies comparison was conducted between rats and humans, focusing on the plasma and urinary pharmacokinetics of GuHong compounds (Figure 3 and Table 1). Another interspecies comparison was conducted for the GuHong compounds through multiple *in vitro*

Table 2

Human pharmacokinetics of circulating Honghua compounds following a 1.5-h intravenous infusion of GuHong (n = 6)

	Day 1		Day 7	
Pharmacokinetic parameter	**Male**	**Female**	**Male**	**Female**
Hydroxysafflor yellow A (1)				
C_{max} (μmol/L)	3.31 ± 0.34	3.67 ± 0.39	3.24 ± 0.37	3.77 ± 0.52
AUC_{0-24h} (h·μmol/L)	14.8 ± 1.20	16.1 ± 2.8	15.5 ± 2.10	17.5 ± 3.10
$AUC_{0-\infty}$ (h·μmol/L)	15.0 ± 1.20	16.5 ± 2.5	15.8 ± 2.20	17.8 ± 3.20
$t_{1/2}$ (h)	4.05 ± 0.28	3.78 ± 0.27	4.28 ± 0.19	4.04 ± 0.28
MRT (h)	5.19 ± 0.20	4.76 ± 0.76	5.37 ± 0.27	5.11 ± 0.28
$CL_{tot,\ p}$ (L/h/kg)	0.03 ± 0.00	0.03 ± 0.00	0.03 ± 0.00	0.03 ± 0.00
V_{SS} (L/kg)	0.15 ± 0.01	0.15 ± 0.01	0.15 ± 0.01	0.15 ± 0.01
CL_R (L/h/kg)	0.03 ± 0.00	0.03 ± 0.00	0.02 ± 0.00	0.03 ± 0.00
f_{e-U} (%)	87.2 ± 6.30	92.0 ± 4.80	79.4 ± 7.20	86.4 ± 10.3
R_{rc}	0.84 ± 0.11	0.97 ± 0.14	0.74 ± 0.13	0.85 ± 0.17
R_{ac}	-	-	1.05	1.08
$f_{u\text{-}plasma}$ (%)	29.7 ± 1.90			
Saffloquinoside D (2)				
C_{max} (μmol/L)	0.35 ± 0.03	0.40 ± 0.04	0.32 ± 0.05	0.38 ± 0.05
AUC_{0-24h} (h·μmol/L)	0.83 ± 0.09	1.04 ± 0.14	0.83 ± 0.13	1.01 ± 0.15
$AUC_{0-\infty}$ (h·μmol/L)	0.90 ± 0.09	1.09 ± 0.15	0.89 ± 0.14	1.06 ± 0.16
$t_{1/2}$ (h)	1.73 ± 0.69	1.64 ± 0.27	1.58 ± 0.21	1.55 ± 0.11
MRT (h)	2.17 ± 0.28	2.42 ± 0.28	2.30 ± 0.17	2.33 ± 0.09
$CL_{tot,\ p}$ (L/h/kg)	0.07 ± 0.00	0.07 ± 0.01	0.07 ± 0.01	0.07 ± 0.01
V_{SS} (L/kg)	0.11 ± 0.02	0.13 ± 0.03	0.12 ± 0.01	0.11 ± 0.01
CL_R (L/h/kg)	0.05 ± 0.01	0.05 ± 0.00	0.06 ± 0.01	0.06 ± 0.01
f_{e-U} (%)	80.2 ± 9.20	86.08 ± 4.4	81.8 ± 9.40	95.6 ± 11.3
R_{rc}	0.63 ± 0.08	0.78 ± 0.09	0.66 ± 0.07	0.90 ± 0.23
R_{ac}	-	-	0.99	0.97
$f_{u\text{-}plasma}$ (%)	70.6 ± 8.3			
Kaempferol-3-*O*-rutinoside (21)				
C_{max} (μmol/L)	0.02 ± 0.00	0.02 ± 0.00	0.02 ± 0.00	0.02 ± 0.01
AUC_{0-24} (h·μmol/L)	0.02 ± 0.00	0.02 ± 0.00	0.02 ± 0.01	0.02 ± 0.00
$AUC_{0-\infty}$ (h·μmol/L)	0.02 ± 0.00	0.02 ± 0.00	0.02 ± 0.01	0.02 ± 0.00
MRT (h)	0.93 ± 0.03	0.97 ± 0.03	0.92 ± 0.02	0.94 ± 0.03
$CL_{tot,\ p}$ (L/h/kg)	1.64 ± 0.21	1.85 ± 0.23	1.69 ± 0.38	1.72 ± 0.23
V_{SS} (L/kg)	0.29 ± 0.05	0.40 ± 0.08	0.30 ± 0.09	0.32 ± 0.08
CL_R (L/h/kg)	0.13 ± 0.04	0.17 ± 0.03	0.16 ± 0.03	0.20 ± 0.04
f_{e-U} (%)	7.87 ± 2.21	9.39 ± 1.19	9.68 ± 2.21	11.4 ± 0.8
R_{rc}	5.48 ± 2.66	5.48 ± 2.66	6.56 ± 2.45	7.11 ± 2.22
R_{ac}	—	—	1.00	1.06
$f_{u\text{-}plasma}$ (%)	24.7 ± 4.9			
Kaempferol-3-*O*-sophoroside (22)				
C_{max} (μmol/L)	0.02 ± 0.00	0.02 ± 0.00	0.02 ± 0.00	0.02 ± 0.01
AUC_{0-24h} (h·μmol/L)	0.02 ± 0.00	0.02 ± 0.00	0.02 ± 0.01	0.02 ± 0.00
$AUC_{0-\infty}$ (h·μmol/L)	0.02 ± 0.00	0.02 ± 0.00	0.02 ± 0.01	0.02 ± 0.00
MRT (h)	0.96 ± 0.02	0.99 ± 0.01	0.95 ± 0.01	0.97 ± 0.03
$CL_{tot,\ p}$ (L/h/kg)	1.09 ± 0.08	1.20 ± 0.11	1.23 ± 0.18	1.12 ± 0.17

(Continued)

Table 2
(Continued)

Pharmacokinetic parameter	Day 1		Day 7	
	Male	Female	Male	Female
V_{SS} (L/kg)	0.17 ± 0.03	0.24 ± 0.05	0.18 ± 0.05	0.19 ± 0.04
CL_R (L/h/kg)	0.14 ± 0.04	0.15 ± 0.03	0.16 ± 0.03	0.16 ± 0.03
$f_{e\text{-}U}$ (%)	12.8 ± 4.10	12.8 ± 2.20	13.3 ± 2.90	14.4 ± 0.80
R_{rc}	2.46 ± 0.61	2.98 ± 0.63	2.91 ± 0.65	3.13 ± 0.52
R_{ac}	—	—	0.89	1.09
$f_{u\text{-}plasma}$ (%)	48.8 ± 3.3			
8-Hydroxycinnamic acid-8-*O*-glucoside (51)				
C_{max} (μmol/L)	0.06 ± 0.01	0.07 ± 0.01	0.05 ± 0.02	0.07 ± 0.01
AUC_{0-24h} (h·μmol/L)	0.07 ± 0.02	0.09 ± 0.02	0.07 ± 0.03	0.10 ± 0.03
$AUC_{0-\infty}$ (h·μmol/L)	0.08 ± 0.02	0.10 ± 0.02	0.08 ± 0.03	0.11 ± 0.03
$t_{1/2}$ (h)	0.25 ± 0.07	0.35 ± 0.16	0.43 ± 0.19	0.38 ± 0.09
MRT (h)	1.05 ± 0.07	1.09 ± 0.07	1.09 ± 0.07	1.09 ± 0.04
$CL_{tot,p}$ (L/h/kg)	1.30 ± 0.22	1.26 ± 0.35	1.38 ± 0.30	1.17 ± 0.27
V_{SS} (L/kg)	0.40 ± 0.10	0.42 ± 0.09	0.46 ± 0.11	0.40 ± 0.11
CL_R (L/h/kg)	0.45 ± 0.13	0.40 ± 0.09	0.42 ± 0.13	0.36 ± 0.10
$f_{e\text{-}U}$ (%)	65.8 ± 9.50	63.0 ± 3.60	61.3 ± 6.70	59.5 ± 4.80
R_{rc}	7.38 ± 2.07	6.60 ± 1.50	7.02 ± 2.21	5.89 ± 1.58
R_{ac}	-	-	0.97	1.07
$f_{u\text{-}plasma}$ (%)	34.2 ± 10.9			
Coumaric acid-4-*O*-glucoside (52)				
C_{max} (μmol/L)	0.13 ± 0.02	0.14 ± 0.02	0.12 ± 0.02	0.14 ± 0.03
AUC_{0-24h} (h·μmol/L)	0.22 ± 0.03	0.25 ± 0.05	0.23 ± 0.04	0.24 ± 0.06
$AUC_{0-\infty}$ (h·μmol/L)	0.31 ± 0.04	0.34 ± 0.06	0.34 ± 0.06	0.32 ± 0.07
$t_{1/2}$ (h)	1.07 ± 0.38	1.19 ± 0.33	1.61 ± 0.80	1.12 ± 0.23
MRT (h)	1.51 ± 0.18	0.57 ± 0.23	1.67 ± 0.40	1.51 ± 0.21
$CL_{tot,p}$ (L/h/kg)	0.13 ± 0.03	0.14 ± 0.02	0.12 ± 0.02	0.14 ± 0.02
V_{SS} (L/kg)	0.12 ± 0.01	0.14 ± 0.02	0.12 ± 0.01	0.13 ± 0.01
CL_R (L/h/kg)	0.12 ± 0.04	0.13 ± 0.03	0.11 ± 0.03	0.13 ± 0.02
$f_{e\text{-}U}$ (%)	90.9 ± 27.5	93.5 ± 25.5	90.5 ± 18.2	93.1 ± 8.50
R_{rc}	1.26 ± 0.51	1.30 ± 0.34	1.12 ± 0.34	1.38 ± 0.26
R_{ac}	-	-	1.04	0.96
$f_{u\text{-}plasma}$ (%)	89.4 ± 15.8			
Chlorogenic acid (53)				
C_{max} (μmol/L)	0.03 ± 0.00	0.03 ± 0.01	0.03 ± 0.00	0.03 ± 0.01
AUC_{0-24h} (h·μmol/L)	0.03 ± 0.01	0.03 ± 0.01	0.03 ± 0.01	0.03 ± 0.01
$AUC_{0-\infty}$ (h·μmol/L)	0.03 ± 0.01	0.03 ± 0.01	0.03 ± 0.01	0.03 ± 0.01
MRT (h)	1.16 ± 0.17	1.17 ± 0.23	0.99 ± 0.11	1.04 ± 0.10
$CL_{tot,p}$ (L/h/kg)	0.56 ± 0.10	0.62 ± 0.10	0.66 ± 0.28	0.64 ± 0.15
V_{SS} (L/kg)	0.21 ± 0.06	0.27 ± 0.16	0.16 ± 0.10	0.19 ± 0.10
CL_R (L/h/kg)	0.30 ± 0.06	0.37 ± 0.07	0.43 ± 0.20	0.47 ± 0.17
$f_{e\text{-}U}$ (%)	54.8 ± 10.8	59.7 ± 4.50	61.1 ± 8.60	68.3 ± 9.70
R_{rc}	4.18 ± 1.18	5.50 ± 0.80	5.81 ± 2.51	6.89 ± 1.90
R_{ac}	—	—	0.89	0.95
$f_{u\text{-}plasma}$ (%)	63.6 ± 7.6			

AUC_{0-t}: Area under the plasma concentration–time curve from 0 to last measurable time point after dosing; $AUC_{0-\infty}$: Area under the plasma concentration-time curve from zero to infinity; C_{max}: Maximum plasma concentration; $CL_{tot,p}$: Total plasma clearance for intravenous administration; CL_R: Renal clearance; $f_{e\text{-}U}$: Fraction of dose excreted into urine; $f_{u\text{-}plasma}$: Unbound fraction in plasma; GFR: Glomerular filtration rate; MRT: Mean residence time; R_{ac}: Accumulation ratio; R_{rc}: Renal clearance ratio; $t_{1/2}$: Elimination half-life; T_{max}: Time taken to achieve C_{max}; V_{SS}: Apparent volume of distribution at steady state for intravenous administration.

Table 3

Net transport ratios of GuHong compounds at 20 μmol/L by human and rat transporters

Transporter	Positive substrate	Hydroxysafflor yellow A (1)	Kaempferol-3-*O*-rutinoside (21)	Kaempferol-3-*O*-sophoroside (22)	8-Hydroxycinnamic acid-8-*O*-glucoside (51)	Coumaric acid-4-*O*-glucoside (52)	Chlorogenic acid (53)	*N*-Acetyl-L-glutamine (81)
Human renal uptake SLC transporters								
OAT1	614 ± 56	1.16 ± 0.37	2.44 ± 1.06	2.55 ± 0.95	5.37 ± 1.42	1.85 ± 0.47	6.70 ± 4.15	1.96 ± 0.21
OAT2	28.7 ± 10.9	1.30 ± 0.25	6.02 ± 2.31	9.58 ± 2.36	9.97 ± 1.24	2.22 ± 0.32	27.1 ± 11.0	1.54 ± 0.52
OAT3	12.2 ± 0.70	0.89 ± 0.01	14.9 ± 8.70	9.96 ± 2.73	41.0 ± 8.70	1.85 ± 0.03	35.6 ± 5.5	0.80 ± 0.15
Human hepatic uptake SLC transporters								
OATP1B1	54.5 ± 0.3	0.81 ± 0.08	16.5 ± 0.2	8.21 ± 1.15	3.14 ± 0.37	1.89 ± 0.47	1.40 ± 0.13	0.48 ± 0.12
OATP1B3	14.7 ± 0.3	1.27 ± 0.39	40.3 ± 2.30	14.9 ± 2.40	35.5 ± 3.50	2.72 ± 0.38	6.03 ± 0.17	0.99 ± 0.42
Human efflux ABC transporters								
MDR1	15.54.1	1.45 ± 0.31	7.85 ± 0.42	5.85 ± 0.21	1.92 ± 0.09	218 ± 25	1.13 ± 0.11	1.06 ± 0.01
BCRP	48.3 ± 4.30	1.04 ± 0.04	10.0 ± 0.50	18.6 ± 0.70	1.90 ± 0.28	231 ± 69	1.19 ± 0.06	1.28 ± 0.04
MRP2	39.8 ± 2.20	2.77 ± 0.33	5.87 ± 0.03	5.51 ± 0.10	1.88 ± 0.27	101 ± 10	1.21 ± 0.17	1.79 ± 0.02
BSEP	6.20 ± 0.51	1.58 ± 0.13	2.08 ± 0.03	1.67 ± 0.14	1.18 ± 0.22	55.8 ± 2.5	1.03 ± 0.05	1.32 ± 0.35
Rat hepatic uptake SLC transporters								
Oatp1b2	32.3 ± 6.5	0.66 ± 0.14	13.7 ± 0.3	6.47 ± 0.19	1.35 ± 0.08	0.59 ± 0.05	0.55 ± 0.17	0.81 ± 0.23
Oat2	8.94 ± 0.04	1.02 ± 0.09	25.4 ± 8.1	24.6 ± 9.1	34.5 ± 2.7	0.95 ± 0.05	6.37 ± 1.73	2.27 ± 0.86
Rat efflux ABC transporters								
Bcrp	80.9 ± 5.1	0.94 ± 0.14	10.5 ± 0.4	25.9 ± 1.6	1.20 ± 0.08	10.9 ± 0.10	1.93 ± 0.06	0.73 ± 0.00
Mrp2	4.20 ± 0.35	0.76 ± 0.04	2.04 ± 0.45	2.47 ± 0.04	0.93 ± 0.04	5.49 ± 0.27	1.58 ± 0.02	0.94 ± 0.24
Bsep	10.9 ± 0.30	1.58 ± 0.06	2.70 ± 0.06	2.84 ± 0.19	1.29 ± 0.04	79.1 ± 0.60	2.73 ± 0.10	0.55 ± 0.07

Human OAT2 is also a hepatic uptake transporter. The positive substrates for OAT1, OAT2/Oat2, OAT3, and OATP1B1/OATP1B3/Oatp1b2 were para-aminohippuric acid, prostaglandin F_{2a}, estrone-3-sulfate, and estradiol-17-β-D-glucuronide, respectively, while those for MDR1, MRP2/Mrp2, BCRP/Bcrp, and BSEP/Bsep were ginsenoside Rg_1, estradiol-17β-D-glucuronide, methotrexate, and taurocholic acid, respectively.

transport studies, using rat and human transporters (Table 3). The rat data indicated that liver exposure to GuHong compounds was not significantly different from the associated systemic exposure. Due to interspecies similarities, a similar pattern is likely to occur in humans. The results of this investigation demonstrate that GuHong does not inhibit or induce the drug-metabolizing enzymes or transporters outlined in the ICH M12 Guideline, indicating that this intravenous herbal medicine has a low potential to precipitate pharmacokinetic drug interactions. The low potential for drug interactions is advantageous for the use of GuHong in the treatment of ischemic stroke, particularly in a polypharmacy context.

In this investigation, seven *in vivo*-exposed compounds derived from the component Honghua were detected in human subjects who intravenously received GuHong. These Honghua compounds are primarily eliminated through renal and/or hepatobiliary excretion, rather than through glucuronidation. Following the recommendations of the ICH M12 Guideline, the potential for drug interactions involving these compounds through the inhibition of uridine diphosphate glucuronosyltransferases (UGTs) was not assessed *in vitro*. This decision also considered the generally limited magnitude of drug interactions mediated by UGT inhibition. Hydroxysafflor yellow A (**1**) is the most significant *in vivo*-exposed Honghua compound, exhibiting a range of properties, including antioxidant, anti-inflammatory, neuroprotective, endothelium-protective, anti-thrombotic, anti-excitotoxic, anti-apoptotic, and autophagy-regulatory effects[57–61]. It was found that **1** exhibited characteristics of a hard drug, being predominantly eliminated through glomerular filtration-based renal excretion in its unchanged form (Table 2). "Hard drugs" refer to pharmacologically active compounds that undergo minimal or no metabolism[62–63]. A key advantage of hard drugs is that they reduce the risk of toxic metabolites and metabolism-based drug interactions. Several *in vivo* metabolites of hydroxysafflor yellow A have been reported in rats, including those formed through oxidation, glucuronidation, sulfation, and glutathione conjugation[64–66]. However, based on the results of the *in vitro* metabolism studies conducted in this study, the reported metabolites were either absent or negligible (Supplementary Figure S1, https://links.lww.com/AHM/A174). In addition, after hydroxysafflor yellow A was administered intravenously to rats at a dose of 1.7 mg/kg, 99.5% of the compound was excreted in the urine, with the reported metabolites being either undetectable or only negligibly present in plasma, urine, or bile samples. The characteristics of hard drugs and glomerular filtration-based renal excretion limit alterations in systemic exposure to **1** through the modulation of drug-metabolizing enzymes and drug transporters, thereby minimizing the risk of this compound being involved in drug interactions as an object. Although L-glutamine is a major metabolite

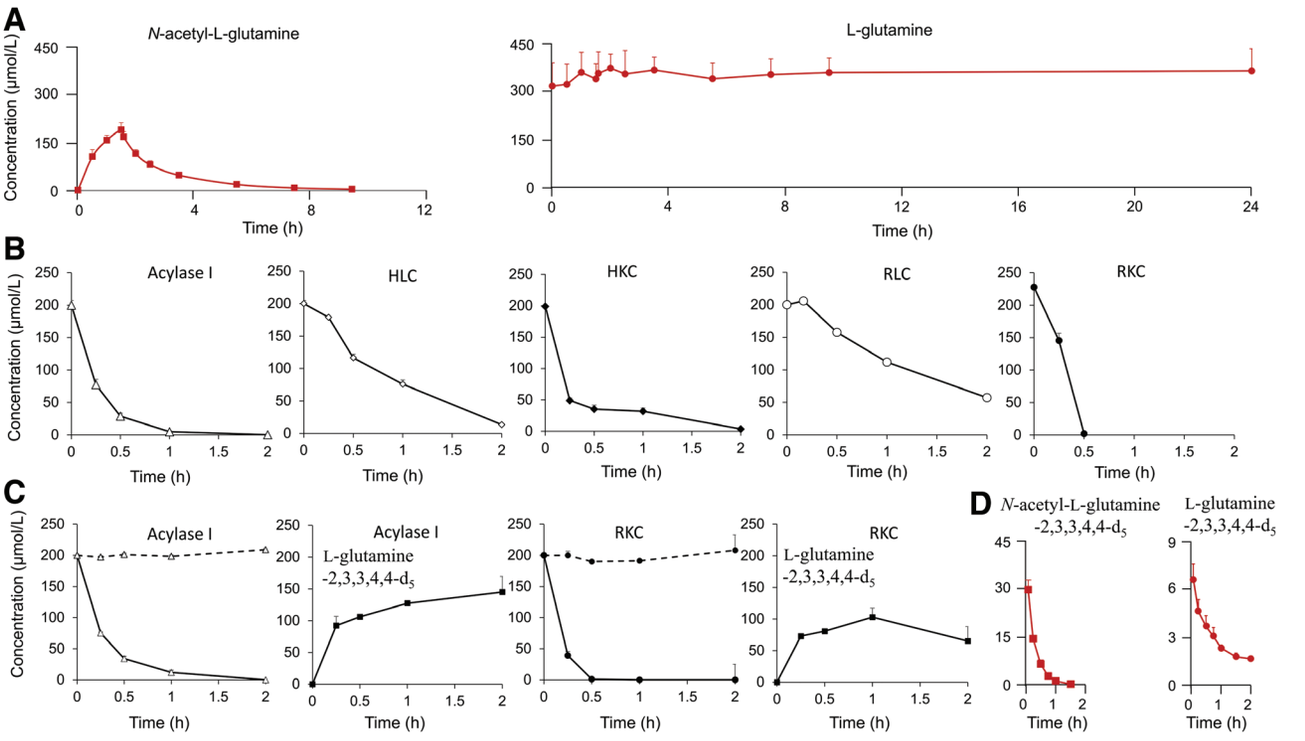


Figure 5. Metabolism of *N*-acetyl-L-glutamine (**81**). (A) Human plasma concentration–time profiles of *N*-acetyl-L-glutamine and L-glutamine following intravenous administration of GuHong; (B) *in vitro* metabolism stability of *N*-acetyl-L-glutamine after incubation with acylase I, HLC, HKC, RLC, and RKC; (C) *in vitro* metabolism of *N*-acetyl-D-glutamine-2,3,3,4,4-d_5 (dashed line) and *N*-acetyl-L-glutamine-2,3,3,4,4-d_5 (solid line) and formation of L-glutamine-2,3,3,4,4-d_5 after incubation with acylase I and rat kidney cytosol; (D) rat plasma concentration–time profiles of *N*-acetyl-L-glutamine-2,3,3,4,4-d_5 and L-glutamine-2,3,3,4,4-d_5 following intravenous administration of *N*-acetyl-DL-glutamine-2,3,3,4,4-d_5. HKC: Human kidney cytosol; HLC: Human liver cytosol; RKC: rat kidney cytosol; RLC: Rat liver cytosol.

of *N*-acetyl-L-glutamine (**81**), no dose-dependent ascending-descending plasma concentration-time profile of L-glutamine was observed in human subjects following intravenous infusion of GuHong. Consequently, L-glutamine was not assessed *in vitro* for its potential to precipitate drug interactions. Given that renal acylase I-mediated hydrolysis to L-glutamine is a major elimination pathway for **81**, the influence of acylase I inhibition or induction on systemic exposure to **81** warrants further evaluation.

Our strategy, which employs a multi-compound pharmacokinetic study, effectively addresses the compound selection challenge and makes the ICH M12 Guideline applicable for assessing the drug interaction potential of complex herbal medicines. Given that the ICH Guideline provides general recommendations for assessing the drug interaction potential of investigational drugs, the resulting drug-enzyme/transporter interaction data require physicians to possess extensive knowledge of drug interactions to guide rational drug therapy, particularly in a polypharmacy context. Therefore, an additional drug interaction assessment is planned for GuHong when used in the management of ischemic stroke, tailored to the stroke patient population and therapeutic context. In further studies, both traditional and non-traditional pharmacokinetic drug interaction potentials will be considered. Traditional pharmacokinetic drug interactions normally involve drug-metabolizing enzyme- or drug transporter–mediated interactions, whereas non-traditional pharmacokinetic drug interactions may involve factors such as disease conditions, lysosomes, intestinal microflora, and other related factors. For example, hydroxysafflor yellow A (**1**) has a small apparent volume of distribution at the steady state (V_{SS}; Table 2), suggesting that this compound is primarily distributed in the plasma and extracellular fluid. Patients with ischemic stroke often experience cerebral edema, which can reduce cerebral exposure to **1** and, consequently, diminish its therapeutic effects. An assessment is required to evaluate the effect of a drug that alleviates stroke-induced edema on the systemic and cerebral exposure to **1**.

In summary, hydroxysafflor yellow A (**1**) is the most prominent *in vivo*-exposed compound originating from the component Honghua in humans following intravenous administration of GuHong, along with six other minor *in vivo*-exposed Honghua flavonoids and phenolic acids. This major *in vivo*-exposed compound, which is primarily eliminated through glomerular filtration-based renal excretion, exhibits pharmacokinetic characteristics typical of a hard drug, thereby minimizing the risk of toxic metabolites and drug interactions (as an object). *N*-acetyl-L-glutamine (**81**) is another major *in vivo*-exposed compound of GuHong. It is primarily eliminated through renal excretion and hydrolyzed to L-glutamine. GuHong has a low potential for precipitating pharmacokinetic drug interactions. This is beneficial for the use of GuHong in the treatment of ischemic stroke, particularly in a polypharmacy context. It is worth noting that these *in vivo*-exposed compounds can be used not only in drug interaction studies but also in pharmacodynamic studies.

Table 4

Human and rat pharmacokinetics of *N*-acetyl-L-glutamine (81) following intravenous administration of GuHong and rat pharmacokinetics of *N*-acetyl-DL-glutamine-2,3,3,4,4-d_5 and L-glutamine-2,3,3,4,4-d_5 following intravenous administration of *N*-acetyl-DL-glutamine-2,3,3,4,4-d_5

Pharmacokinetic parameter	N-Acetyl-L-glutamine (81)	
Human data of *N*-acetyl-$_L$-glutamine (following a 1.5-h intravenous infusion of GuHong, *n* = 6)		
	Day 1	**Day 7**
C_{max} (μmol/L)	191 ± 30	211 ± 32
$AUC_{0–24h}$ (h·μmol/L)	460 ± 64	524 ± 76
$AUC_{0–\infty}$ (h·μmol/L)	465 ± 64	531 ± 77
$t_{1/2}$ (h)	1.63 ± 0.20	1.90 ± 0.21
MRT (h)	1.78 ± 0.12	1.77 ± 0.12
$CL_{tot,\ p}$ (L/h/kg)	0.11 ± 0.01	0.10 ± 0.01
V_{SS} (L/kg)	0.20 ± 0.02	0.17 ± 0.01
CL_R (L/h/kg)	0.04 ± 0.01	0.03 ± 0.01
$f_{e\text{-}U}$ (%)	36.1 ± 6.1	34.2 ± 6.0
R_{rc}	0.32 ± 0.06	0.27 ± 0.06
R_{ac}	1.15	1.13
$f_{u\text{-}plasma}$ (%)	99.7 ± 3.5	
Rat data of *N*-acetyl-$_L$-glutamine (iv bolus dose of GuHong, *n* = 6)		
C_{max} (μmol/L)	833 ± 119	
$AUC_{0–24h}$ (h·μmol/L)	315 ± 20	–
$AUC_{0–\infty}$ (h·μmol/L)	315 ± 20	–
$t_{1/2}$ (h)	0.23 ± 0.02	–
MRT (h)	0.30 ± 0.02	–
$CL_{tot,\ p}$ (L/h/kg)	1.02 ± 0.06	–
V_{SS} (L/kg)	0.30 ± 0.03	–
Rat data of *N*-acetyl-DL-glutamine-2,3,3,4,4-d_5 and L-glutamine-2,3,3,4,4-d_5 (following iv bolus dose of *N*-acetyl-DL-glutamine-2,3,3,4,4-d_5, *n* = 3)		
	N-acetyl-DL-glutamine-2,3,3,4,4-d5	**L-glutamine-2,3,3,4,4-d5**
C_{max} (μmol/L)	29.5 ± 3.1	6.63 ± 0.94
$AUC_{0–24h}$ (h·μmol/L)	10.9 ± 1.2	7.90 ± 0.51
$AUC_{0–\infty}$ (h·μmol/L)	11.0 ± 1.2	8.56 ± 0.48
$t_{1/2}$ (h)	0.17 ± 0.03	1.14 ± 0.05
MRT (h)	0.27 ± 0.02	1.57 ± 0.09
$CL_{tot,\ p}$ (L/h/kg)	0.61 ± 0.08	–
V_{SS} (L/kg)	0.16 ± 0.01	–

Although L-glutamine is the metabolite of *N*-acetyl-L-glutamine (81), no distinct dose-dependent ascending-descending plasma concentration-time profile of L-glutamine was observed in human subjects or rats following an intravenous infusion of GuHong.

Conflict of interest statement

The authors declare no conflict of interest.

Funding

This work was supported in part by the National Natural Science Foundation of China Grants (82192912 and 82074273) and by the National Key R&D Program ("Strategic Scientific and Technological Innovation Cooperation") Key Project (2022YFE0203600) released by the Ministry of Science and Technology.

Author contributions

Chuan Li and Jun-Ling Yang designed the study. Chuan Li, Jun-Ling Yang, and Qiu-Yue Wang wrote the paper. Qiu-Yue Wang, Jun-Ling Yang, Zhen-Zhen Ma, Jia-Ye Yuan, Guo-Li Yue, Yun-Fei Feng, Xiao-Yan Xia, Wei-Wei Jia, Fei-Fei Du, Feng-Qing Wang, Xuan Yu, Chen Cheng, Yü-Hong Huang, Yi-Mei Zeng, and Yan-Fen Li conducted the study. Xiao-Kai Wang contributed new reagents. Chuan Li, Jun-Ling Yang, Qiu-Yue Wang, Xiao-Kai Wang, and Zi-Jing Song analyzed the data. All the authors have read and approved the final version of the manuscript.

Table 5

Inhibitory effects of *in vivo*-exposed GuHong compounds on human drug-metabolizing enzymes and drug transporters

		Percentage inhibition by GuHong compounds of human drug-metabolizing enzymes and transporters							
Drug-metabolizing enzymes [substrate → metabolite] or transporters [substrate]	**Percentage inhibition by positive inhibitor**	**Hydroxysafflor yellow A (1)**	**Kaempferol-3-*O*-rutinoside (21)**	**Kaempferol-3-*O*-sophoroside (22)**	**8-Hydroxycinnamic acid-8-*O*-glucoside (51)**	**Coumaric cid-4-*O*-glucoside (52)**	**Chlorogenic acid (53)**	***N*-Acetyl-L-glutamine (81)**	**MGHC**
CYP1A2 [phenacetin → acetaminophen]	74.0 ± 1.9	4.67 ± 3.08	0	0	0	0	0	2.08 ± 2.38	0
CYP2B6 [bupropion → hydroxybupropion]	98.6 ± 1.1	16.1 ± 1.1	6.70 ± 0.99	8.09 ± 1.39	6.95 ± 1.23	6.30 ± 4.05	9.24 ± 3.63	24.2 ± 5.1	23.3 ± 4.1
CYP2C8 [amodiaquine → desethylamodiaquine]	76.7 ± 1.8	11.3 ± 3.5	22.6 ± 2.6	25.9 ± 5.3	16.1 ± 2.5	14.1 ± 2.9	14.8 ± 9.4	43.6 ± 9.6	0
CYP2C9 [diclofenac → 4'-hydroxydiclofenac]	97.3 ± 1.6	17.5 ± 13.1	6.88 ± 6.62	0	4.66 ± 0.49	11.5 ± 5.4	15.2 ± 6.9	5.30 ± 8.31	24.2 ± 9.9
CYP2C19 [*S*-mephenytoin → 4'-hydroxymephenytoin]	96.8 ± 0.2	35.7 ± 6.4	20.0 ± 4.7	22.6 ± 3.6	2.14 ± 0.94	8.51 ± 4.34	18.0 ± 2.5	14.6 ± 2.3	3.60 ± 5.00
CYP2D6 [dextromethorphan → dextrorphan]	98.6 ± 2.5	31.4 ± 9.3	5.46 ± 7.31	2.33 ± 2.44	0	4.09 ± 6.60	0	12.0 ± 13.6	9.36 ± 13.4
CYP3A [midazolam → 1'-hydroxymidazolam]	93.6 ± 0.1	44.5 ± 12.1	17.4 ± 9.7	9.69 ± 4.40	0	12.6 ± 2.4	4.80 ± 6.31	10.6 ± 5.7	23.2 ± 8.7
CYP3A [testosterone → 6β-hydroxytestosterone]	98.8 ± 2.0	0	0	0	11.4 ± 18.5	0	0	37.9 ± 1.9	16.3 ± 16.1
OATP1B1 [estradiol-17 β-D-glucuronide]	100 ± 0	18.5 ± 8.8	8.65 ± 8.61	26.2 ± 7.4	15.9 ± 5.1	6.64 ± 4.88	9.69 ± 1.99	21.1 ± 7.5	21.2 ± 6.6
OATP1B3 [estradiol-17 β-D-glucuronide]	100 ± 0	24.9 ± 6.9	10.4 ± 11.5	13.7 ± 4.9	17.6 ± 11.4	24.4 ± 3.6	26.1 ± 7.1	28.0 ± 7.7	23.0 ± 13.9
OAT1 [*para*-aminohippuric acid]	99.0 ± 0.1	11.2 ± 1.0	0	12.3 ± 1.7	0	0	0	4.38 ± 0.94	0
OAT3 [estrone-3-sulfate]	71.6 ± 0.6	0	9.09 ± 1.20	14.4 ± 8.5	16.6 ± 2.6	26.6 ± 2.5	19.7 ± 4.8	9.63 ± 4.62	16.3 ± 1.9
OCT2 [tetraethylammonium]	79.0 ± 8.2	25.1 ± 2.0	2.37 ± 5.42	1.64 ± 2.32	0	4.62 ± 8.01	31.6 ± 9.6	40.3 ± 13.6	5.66 ± 5.42
MATE1 [tetraethylammonium]	99.0 ± 0.2	22.2 ± 2.8	3.42 ± 5.92	0	3.70 ± 2.37	5.13 ± 4.24	13.0 ± 11.9	26.5 ± 4.8	14.9 ± 4.5
MATE2K [tetraethylammonium]	59.4 ± 5.3	31.8 ± 6.9	15.8 ± 7.7	25.8 ± 5.7	23.7 ± 4.0	13.3 ± 11.3	21.4 ± 9.8	9.98 ± 11.62	17.9 ± 12.6
MDR1 [ginsenoside Rg_1]	86.9 ± 0.2	12.1 ± 1.6	25.2 ± 2.3	16.9 ± 0.4	3.33 ± 4.71	39.7 ± 2.5	32.1 ± 2.2	37.9 ± 4.7	35.2 ± 16.4
BCRP [methotrexate]	100 ± 0	0	35.5 ± 10.8	11.1 ± 11.9	2.51 ± 3.56	5.18 ± 7.32	0	0	0

BCRP: Breast cancer resistance protein; MATE: Multidrug and toxin extrusion protein; MDR: Multidrug resistance; MGHC: Mixture of GuHong compounds; OAT: Organic anion transporter; OATP: Organic anion-transporting polypeptide; OCT: Organic cation transporter.

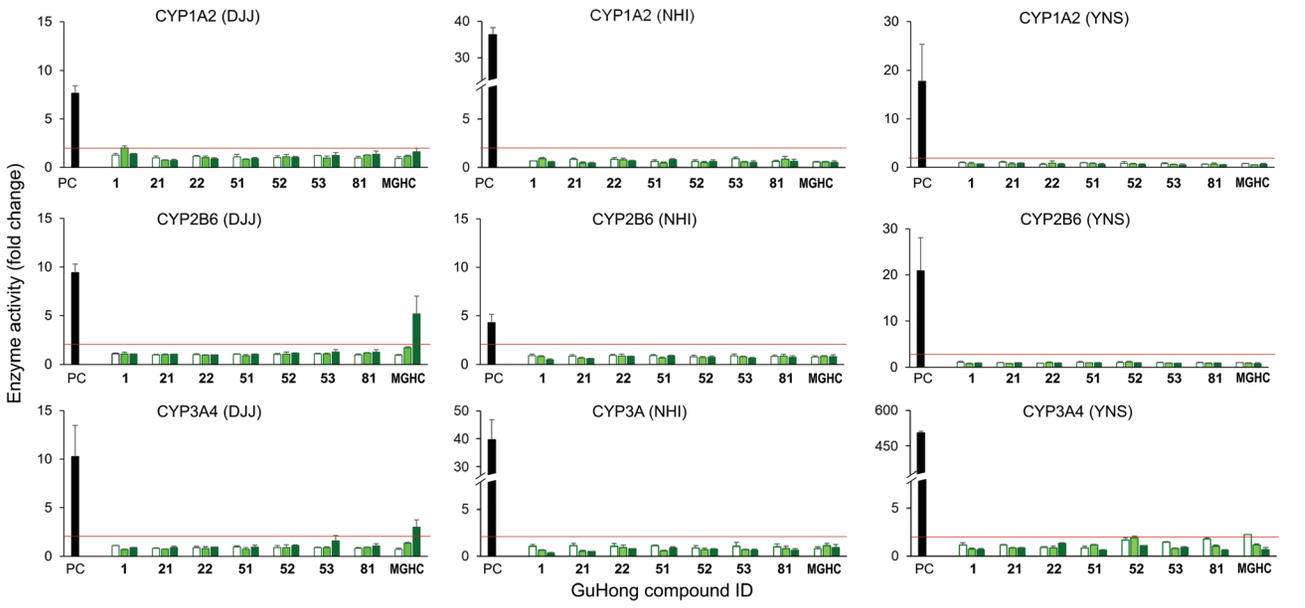


Figure 6. Induction of P450s by *in vivo*-exposed GuHong compounds at three concentrations [unbound C_{max} × 1 (open bars), ×5 (light green bars), and ×50 (green bars)] in cryopreserved human hepatocytes from three donors (DJJ, NHI, and YNS). Phenacetin, bupropion, and midazolam were used as probe substrates for CYP1A2, CYP2B6, and CYP3A, respectively. Omeprazole, phenobarbital, and rifampin were used as PC for CYP1A2, CYP2B6, and CYP3A, respectively. Data are expressed as the mean ± SD (n = 3). PC: Positive controls; SD: Standard deviation.

Ethical approval of studies and informed consent

The human study protocol was reviewed and approved by the hospital's Ethics Committee of Clinical Investigation (2021-008-01). The volunteers provided written informed consent before enrollment. The animal research protocols were reviewed and approved by the Institutional Animal Care and Use Committee of the Shanghai Institute of Materia Medica (2020-10-LC-33).

Acknowledgments

None.

Data availability

The datasets generated and/or analyzed in the current study are available from the corresponding author upon reasonable request.

References

[1] Wang C, Cao B, Liu Q-Q, et al. Oseltamivir compared with the Chinese traditional therapy maxingshigan-yinqiaosan in the treatment of H1N1 influenza: a randomized trial. *Ann Intern Med* 2011;155(4):217–225.
[2] Li X-L, Zhang J, Huang J, et al. A multicenter, randomized, double-blind, parallel-group, placebo-controlled study of the effects of qili qiangxin capsules in patients with chronic heart failure. *J Am Coll Cardiol* 2013;62(12):1065–1072.
[3] Lam W, Bussom S, Guan F-L, et al. The four-herb Chinese medicine PHY906 reduces chemotherapy-induced gastrointestinal toxicity. *Sci Transl Med* 2010;2(45):45ra59.
[4] Zhang L, Li P, Xing C-Y, et al. Efficacy and safety of *Abelmoschus manihot* for primary glomerular disease: a prospective, multicenter randomized controlled clinical trial. *Am J Kidney Dis* 2014;64(1):57–65.
[5] Song Y-L, Yao C, Yao Y-M, et al. XueBiJing injection versus placebo for critically ill patients with severe community-acquired pneumonia: a randomized controlled trial. *Crit Care Med* 2019;47:e735–e743.
[6] Liu S-Q, Yao C, Xie J-F, et al. Effect of XueBiJing injection on 28-day mortality in patients with sepsis: the EXIT-SEP randomized clinical trial. *JAMA Intern Med* 2023;183:647–655.
[7] Yang Y-J, Li X-D, Chen G-H, et al. Traditional Chinese medicine compound (Tongxinluo) and clinical outcomes of patients with acute myocardial infarction: the CTS-AMI randomized clinical trial. *JAMA* 2023;330(16):1534–1545.
[8] Zhao J, Tostivint I, Xu L-D, et al. Efficacy of combined *Abelmoschus manihot* and irbesartan for reduction of albuminuria in patients with type 2 diabetes and diabetic kidney disease: a multicenter randomized double-blind parallel controlled clinical trial. *Diabetes Care* 2022;45(7):e113–e115.
[9] Li J, Olaleye OE, Yu X, et al. High degree of pharmacokinetic compatibility exists between the five-herb medicine XueBiJing and antibiotics comedicated in sepsis care. *Acta Pharm Sin B* 2019;9(5):1035–1049.
[10] Li C, Jia W-W, Yang J-L, et al. Multi-compound and drug-combination pharmacokinetic research on Chinese herbal medicines. *Acta Pharmacol Sin* 2022;43(12):3080–3095.
[11] Bailey DG, Spence JD, Munoz C, et al. Interaction of citrus juices with felodipine and nifedipine. *Lancet* 1991;337:268–269.
[12] Bailey DG, Arnold JMO, Bend JR, et al. Grapefruit juice–felodipine interaction: reproducibility and characterization with the extended release drug formulation. *Br J Clin Pharmacol* 1995;40:135–140.
[13] Ruschitzka F, Meier PJ, Turina M, et al. Acute heart transplant rejection due to Saint John's wort. *Lancet* 2000;355:548–549.
[14] Breidenbach T, Kliem V, Burg M, et al. Profound drop of cyclosporine a whole blood trough levels caused by St. John's wort (*Hypericum perforatum*). *Transplantation* 2000;69:2229–2230.
[15] Moore LB, Goodwin B, Jones SA, et al. St. John's wort induces hepatic drug metabolism through activation of the pregnane X receptor. *Proc Natl Acad Sci USA* 2000;97(13):7500–7502.
[16] Nicolussi S, Drewe J, Butterweck V, et al. Clinical relevance of St. John's wort drug interactions revisited. *Br J Pharmacol* 2020;177(6):1212–1226.
[17] Shaikh AS, Thomas AB, Chitlange SS. Herb-drug interaction studies of herbs used in treatment of cardiovascular disorders-a narrative review of preclinical and clinical studies. *Phytother Res* 2020;34(5):1008–1026.
[18] Thikekar AK, Thomas AB, Chitlange SS. Herb-drug interactions in diabetes mellitus: a review based on pre-clinical and clinical data. *Phytother Res* 2021;35(9):4763–4781.
[19] Hu Z-P, Yang X-X, Ho PC, et al. Herb-drug interactions: a literature review. *Drugs* 2005;65(9):1239–1282.
[20] Ye L, Fan S-C, Zhao P-F, et al. Potential herb-drug interactions between anti-COVID-19 drugs and traditional Chinese medicine. *Acta Pharm Sin B* 2023;13(9):3598–3637.
[21] Zhang Y-F, Man Ip C, Lai YS, et al. Overview of current herb-drug interaction databases. *Drug Metab Dispos* 2022;50(1):86–94.

[22] Li M-T, Wang Y-L, Chen Y, et al. A comprehensive review on pharmacokinetic mechanism of herb-herb/drug interactions in Chinese herbal formula. *Pharmacol Ther* 2024;264:108728.
[23] Li C. Multi-compound pharmacokinetic research on Chinese herbal medicines: approach and methodology. *China J Chin Mater Med* 2017;42(4):607–617.
[24] Li C, Cheng C, Jia W-W, et al. Multi-compound pharmacokinetic research on Chinese herbal medicines: identifying the medicines' potentially therapeutic compounds and characterizing their disposition and pharmacokinetics. *Acta Pharm Sin* 2021;56(9):2426–2446.
[25] Olaleye OE, Niu W, Du F-F, et al. Multiple circulating saponins from intravenous ShenMai inhibit OATP1Bs *in vitro*: potential joint precipitants of drug interactions. *Acta Pharmacol Sin* 2018;40(6):833–849.
[26] Pintusophon S, Niu W, Duan X-N, et al. Intravenous formulation of Panax notoginseng root extract: human pharmacokinetics of ginsenosides and potential for perpetrating drug interactions. *Acta Pharmacol Sin* 2019;40(10):1351–1363.
[27] Xia J, Yin J, Xiong T, et al. Clinical efficacy and safety of guhong injection in treatment of acute ischemic stroke: a multicenter, randomized, double-blind, placebo-controlled clinical trial. *J Int Neurol Neurosur* 2024;51(4):1–7.
[28] Zhang W-W, Xin J, Zhang G-Y, et al. Efficacy of Guhong injection versus Butylphthalide and Sodium Chloride Injection for mild ischemic stroke: a multicenter controlled study. *World J Clin Cases* 2022;10(21):7265–7274.
[29] Wang Y-L, Wu H-M, Han Z, et al. Guhong injection promotes post-stroke functional recovery *via* attenuating cortical inflammation and apoptosis in subacute stage of ischemic stroke. *Phytomedicine* 2022;99:154034.
[30] Wang Y-L, Wu H-M, Sheng H-D, et al. Discovery of anti-stroke active substances in Guhong injection based on multi-phenotypic screening of zebrafish. *Biomed Pharmacother* 2022;155:113744.
[31] Zhou Z-H, Lu J-F, Liu W-W, et al. Advances in stroke pharmacology. *Pharmacol Ther* 2018;191:23–42.
[32] Wang Q-Y, Yang Z-H, Guo L-L, et al. Chemical composition, pharmacology and pharmacokinetic studies of GuHong injection in the treatment of ischemic stroke. *Front Pharmacol* 2023;14:1261326.
[33] Shi X-H, Tang Y-H, Chen J-Z, et al. Pharmacokinetics of hydroxysafflor yellow A in Guhong Injection in rats. *Chin Tradit Pat Med* 2015;37(11):2387–2391.
[34] Chen J-K, Wan H-T, Zhou H-F, et al. Correlation study on *in vivo* pharmacokinetics and anti-oxidation of Guhong Injection in cerebral ischemia reperfusion injury model of rats. *Chin Tradit Herb Drugs* 2016;47(3):447–453.
[35] Yu L, Wan H-F, Li C, et al. Pharmacokinetics of active components from Guhong injection in normal and pathological rat models of cerebral ischemia: a comparative study. *Front Pharmacol* 2018;9:493.
[36] Xu S-C, Li C, Zhou H-F, et al. A study on acetylglutamine pharmacokinetics in rat blood and brain based on liquid chromatography-tandem mass spectrometry and microdialysis technique. *Front Pharmacol* 2020;11:508.
[37] Cheng C, Ren C, Li M-Z, et al. Pharmacologically significant constituents collectively responsible for anti-sepsis action of XueBiJing, a Chinese herb-based intravenous formulation. *Acta Pharmacol Sin* 2024;45:1077–1092.
[38] Yu X, Niu W, Wang Y-Y, et al. Novel assays for quality evaluation of XueBiJing: quality variability of a Chinese herbal injection for sepsis management. *J Pharm Anal* 2022;12(4):664–682.
[39] Li M-J, Wang F-Q, Huang Y-H, et al. Systemic exposure to and disposition of catechols derived from *Salvia miltiorrhiza* roots (Danshen) after intravenous dosing DanHong injection in human subjects, rats, and dogs. *Drug Metab Dispos* 2015;43(5):679–690.
[40] Cheng C, Du F-F, Yu K, et al. Pharmacokinetics and disposition of circulating iridoids and organic acids in rats intravenously receiving ReDuNing injection. *Drug Metab Dispos* 2016;44(11):1853–1858.
[41] Cheng C, Lin J-Z, Li L, et al. Pharmacokinetics and disposition of monoterpene glycosides derived from *Paeonia lactiflora* roots (Chishao) after intravenous dosing of antiseptic XueBiJing injection in human subjects and rats. *Acta Pharmacol Sin* 2016;7:530–544.
[42] Zhang N-T, Cheng C, Olaleye OE, et al. Pharmacokinetics-based identification of potential therapeutic phthalides from XueBiJing, a Chinese herbal injection used in sepsis management. *Drug Metab Dispos* 2018;46:823–834.
[43] Zhang H-Y, Wang Q-Y, Wang J-N, et al. Composition analysis of Compound Shenhua Tablet, a seven-herb Chinese medicine for IgA nephropathy: evaluation of analyte-capacity of the assays. *Chin J Nat Med* 2024;22(2):178–192.
[44] Chen F, Li L, Xu F, et al. Systemic and cerebral exposure to and pharmacokinetics of flavonols and terpene lactones after dosing standardized *Ginkgo biloba* leaf extracts to rats *via* different administration routes. *Br J Pharmacol* 2013;170:440–457.
[45] Reagan-Shaw S, Nihal M, Ahmad N. Dose translation from animal to human studies revisited. *FASEB J* 2008;22(3):659–661.
[46] Jia W-W, Du F-F, Liu X-W, et al. Renal tubular secretion of tanshinol: molecular mechanisms, impact on its systemic exposure, and propensity for dose-related nephrotoxicity and for renal herb-drug interactions. *Drug Metab Dispos* 2015;43(5):669–678.
[47] Jiang R-R, Dong J-J, Li X-X, et al. Molecular mechanisms governing different pharmacokinetics of ginsenosides and potential for ginsenoside-perpetrated herb-drug interactions on OATP1B3. *Br J Pharmacol* 2015;172(4):1059–1073.
[48] Grimm SW, Einolf HJ, Hall SD, et al. The conduct of *in vitro* studies to address time-dependent inhibition of drug metabolizing enzymes: a perspective of the pharmaceutical research and manufacturers of America. *Drug Metab Dispos* 2009;37(7):1355–1370.
[49] Zhong C-C, Chen F, Yang J-L, et al. Pharmacokinetics and disposition of anlotinib, an oral tyrosine kinase inhibitor, in experimental animal species. *Acta Pharmacol Sin* 2018;39(6):1048–1063.
[50] Zhou X-D, Tang L-Y, Xu Y-L, et al. Towards a better understanding of medicinal uses of Carthamus *tinctorius* L. in traditional Chinese medicine: a phytochemical and pharmacological review. *J Ethnopharmacol* 2014;151(1):27–43.
[51] Zhang L-L, Tian K, Tang Z-H, et al. Phytochemistry and pharmacology of *Carthamus tinctorius* L. *Am J Chin Med* 2016;44(2):197–226.
[52] Xian B, Wang R, Jiang H-J, et al. Comprehensive review of two groups of flavonoids in *Carthamus tinctorius* L. *Biomed Pharmacother* 2022;153:113462.
[53] Yang W-Z, Si W, Zhang J-X, et al. Selective and comprehensive characterization of the quinochalcone C-glycoside homologs in *Carthamus tinctorius* L. by offline comprehensive two-dimensional liquid chromatography/LTQ-Orbitrap MS coupled with versatile data mining strategies. *RSC Adv* 2016;6:495–506.
[54] Yao C-L, Yang W-Z, Si W, et al. An enhanced targeted identification strategy for the selective identification of flavonoid *O*-glycosides from *Carthamus tinctorius* by integrating offline two-dimensional liquid chromatography/linear ion-trap-Orbitrap mass spectrometry, high-resolution diagnostic product ions/neutral loss filtering and liquid chromatography-solid phase extraction-nuclear magnetic resonance. *J Chromatogr A* 2017;1491:87–97.
[55] Lan X-F, Olajide OE, Du F-F, et al. Pharmacokinetics-based identification of pseudoaldosterogenic compounds originating from *Glycyrrhiza uralensis* roots (Gancao) after dosing LianhuaQingwen capsule. *Acta Pharmacol Sin* 2021;42:2155–2172.
[56] Tian D-D, Jia W-W, Liu X-W, et al. Methylation and its role in disposition of tanshinol, a cardiovascular carboxylic catechol from Salvia miltiorrhiza roots (Danshen). *Acta Pharmacol Sin* 2015;36:627–643.
[57] Bai X, Wang W-X, Fu R-J, et al. Therapeutic potential of hydroxysafflor yellow A on cardio-cerebrovascular diseases. *Front Pharmacol* 2020;11:01265.
[58] Li Y, Liu X-T, Zhang P-L, et al. Hydroxysafflor yellow A blocks HIF-1 α induction of NOX2 and protects ZO-1 protein in cerebral microvascular endothelium. *Antioxidants (Basel)* 2022;11(4):728.
[59] Yu L, Jin Z, Li M-C, et al. Protective potential of hydroxysafflor yellow A in cerebral ischemia and reperfusion injury: an overview of evidence from experimental studies. *Front Pharmacol* 2022;13:1063035.
[60] Zhang Y-L, Liu Y, Cui Q, et al. Hydroxysafflor yellow A alleviates ischemic stroke in rats *via* HIF-1α, BNIP3, and Notch1-Mediated inhibition of autophagy. *Am J Chin Med* 2022;50(3):799–815.
[61] Lai Z-L, Li C, Ma H-H, et al. Hydroxysafflor yellow A confers neuroprotection against acute traumatic brain injury by modulating neuronal autophagy to inhibit NLRP3 inflammasomes. *J Ethnopharmacol* 2023;308:116268.
[62] Ariëns EJ. Excursions in the field of SAR: a consideration of the past, the present and the future. In: Keverling Buiman JA, ed. *Biological Activity and Chemical Structure*. Elsevier; 1972. pp 1–35.

[63] Ariëns EJ, Simonis AM. Optimalisation of pharmacokinetics: an essential aspect of drug development-by "metabolic stabilisation." In: Keverling Buiman JA, ed. *Strategy in Drug Research*. Elsevier; 1982. pp 165–178.
[64] Li J-R, Sun M-J, Ping Q-N, et al. Metabolism, excretion and bioavailability of hydroxysafflor Yellow A after oral administration of its lipid-based formulation and aqueous solution in rats. *Chin J Nat Med* 2010;8(3):233–240.
[65] Jin Y, Wu L, Tang Y-P, et al. UFLC-Q-TOF/MS based screening and identification of the metabolites in plasma, bile, urine and feces of normal and blood stasis rats after oral administration of hydroxysafflor yellow A. *J Chromatogr B Analyt Technol Biomed Life Sci* 2016;1012–1013:124–129.
[66] Wu L, Tang Y, Shan C, et al. A comprehensive *in vitro* and *in vivo* metabolism study of hydroxysafflor yellow A. *J Mass Spectrom* 2018;53(2):99–108.